

CONTENTS — J through L

Short-lived Nuclides and the Origin of the Solar System <i>S. B. Jacobsen</i>	5217
Continued Isotopic Studies of Presolar Graphite from Orgueil <i>M. Jadhav, S. Amari, E. Zinner, and T. Maruoka</i>	5303
SAHARA 03500: A Unique Achondrite <i>A. Jambon and B. Devouard</i>	5272
Heterogeneous Th-U-Pb Isotope and Elemental Systematics in Calcium-Aluminum-rich Inclusions Determined by LA-ICPMS <i>K. P. Jochum, J. M. Friedrich, D. S. Ebel, and S. J. G. Galer</i>	5108
Synthesizing Organics Using Amorphous Mg- and Fe- Silicate Grains <i>N. M. Johnson, M. Martin, J. P. Dworkin, and J. A. Nuth III</i>	5242
South Pole-Aitken Basin and the Composition of the Lunar Crust <i>B. L. Jolliff and J. J. Gillis</i>	5330
Calculations of Lunar Bulk Composition <i>J. H. Jones</i>	5035
Studies of ^{14}C and ^{10}Be Production Rates and Terrestrial Ages of Desert Meteorites <i>A. J. T. Jull, L. R. McHargue, K. J. Kim, J. A. Johnson, P. A. Bland, and A. W. R. Bevan</i>	5181
Spectrum Imaging of Space-weathered Rims on Lunar Soil Grains <i>L. P. Keller and R. Christoffersen</i>	5244
Quantitative Reanalysis of Near-Infrared Data for Asteroid 4953 1990 MU <i>M. S. Kelley and M. J. Gaffey</i>	5333
Geochemistry, Mineralogy, and Weathering of the Antarctic Ferrar Dolerite with Implications for Martian Meteorites and Surface Processes <i>J. D. Kennedy and R. P. Harvey</i>	5232
The Effects of Geometry on Nuclide Production Processes in Meteorites <i>K. J. Kim, J. Masarik, and R. C. Reedy</i>	5262
The Stratigraphic and Historic Record of Meteoritic Impact Events in Alabama <i>D. T. King Jr. and L. W. Petruny</i>	5317
Target-affected Morphology of the Wetumpka (Marine) Impact Crater, USA <i>D. T. King Jr., J. Ormö, L. W. Petruny, J. R. Morrow, R. C. Johnson, and T. L. Neathery</i>	5301
Early Solar System Granites <i>P. L. King, K. D. Dalby, S. D. J. Russell, T. Ireland, H. Y. McSween Jr., and A. Bischoff</i>	5260
Internal Heating of the Ureilite Parent Body by Short-lived Nuclides <i>N. T. Kita, Y. Ikeda, G. Shimoda, S. Togashi, Y. Morisihita, and M. K. Weisberg</i>	5178
Magnetic Paleofield Estimates for Chondrules Extracted from the Bjurböle (L4) Meteorite <i>G. Kletetschka, P. T. Wasilewski, and V. Zila</i>	5150

Tektites: Why are They on the Earth, but Not on the Moon? <i>C. Koeberl</i>	5069
Discriminating Glasses and Phyllosilicates in Thermal Infrared Data <i>W. C. Koeppen and V. E. Hamilton</i>	5144
The Global Distribution of Olivine on Mars: Forsterite to Fayalite <i>W. C. Koeppen and V. E. Hamilton</i>	5143
Chondrule Magnetic Conglomerate Test of Avanhandava H4 Chondrite <i>T. Kohout and L. J. Pesonen</i>	5202
Crystallization of Lunar Mare Meteorite LAP 02205 <i>E. Koizumi, J. Chokai, T. Mikouchi, J. Makishima, and M. Miyamoto</i>	5152
Geochemical Evidence for the Novaya Yerga Meteorite Fall, 1660 <i>A. V. Korochantsev, C. A. Lorenz, M. A. Ivanova, and M. A. Nazarov</i>	5179
The Myth of the Magnesian Suite of Lunar "Highlands" Rocks <i>R. L. Korotev</i>	5052
Ion Implantation into Nanodiamonds and the Mechanism of High Temperature Release of Noble Gases from Meteoritic Diamonds <i>A. P. Koscheev, M. D. Gromov, P. V. Gorokhov, U. Ott, G. R. Huss, and T. L. Daulton</i>	5337
Coarse-grained Anorthite-rich (Type C) CAIs in Carbonaceous Chondrites: Evidence for a Complex Formation History <i>A. N. Krot, H. Yurimoto, M. I. Petaev, I. D. Hutcheon, D. A. Wark, G. Libourel, L. Tissandier, and J. M. Paque</i>	5256
Lunar Feldspathic Meteorite NWA 2200; A Polymict Glassy Impact-Melt Breccia with Ferroan Anorthosite (FAN) Affinities <i>S. M. Kuehner, A. J. Irving, and D. A. Gregory</i>	5137
Trace Element Abundances in St. Aubin (UNGR Iron) Giant Chromite and Associated Phases <i>G. Kurat, E. Zinner, and M. E. Varela</i>	5087
A Zoned Spinel Grain in the Fountain Hills Bencubbinite: Constraints on Its Thermal History <i>A. R. La Blue, D. S. Lauretta, and M. Killgore</i>	5273
Mössbauer Study of Iron Phosphides Extracted from Sikhote-Alin Meteorite <i>M. Yu. Larionov, V. I. Grokhovsky, and M. I. Oshtrakh</i>	5086
The Fountain Hills Bencubbinite: A Record of Chondrule Formation in High Temperature Regions of the Solar Nebula <i>D. S. Lauretta, A. R. La Blue, and M. Killgore</i>	5275
The Lunar Prospector Gamma-Ray and Neutron Spectrometers: Overview of Lunar Global Composition Measurements <i>D. J. Lawrence, R. C. Elphic, W. C. Feldman, O. Gasnault, J. J. Hagerty, S. Maurice, and T. H. Prettyman</i>	5210
Multiple Nakhilite Lava Flows? <i>R. C. F. Lentz, T. J. McCoy, and G. J. Taylor</i>	5298

Noble Gases in Meteorite Showers from Queen Alexandra Range and Frontier Mountain <i>I. Leya and K. C. Welten</i>	5082
Titanium Isotopes in the Solar System <i>I. Leya, M. Schönbächler, U. Wiechert, and A. N. Halliday</i>	5081
Major, Trace and Platinum-Group Elements of the Martian Lherzolite Grove Mountains (GRV) 99027 <i>Y. T. Lin, L. Qi, G. Q. Wang, and L. Xu</i>	5154
Re-Examination of ²⁶ Al Abundance in CM Hibonite Grains <i>M.-C. Liu and K. D. McKeegan</i>	5304
Morphologies of Apollo 17 Dust and Lunar Simulant JSC-1 <i>Y. Liu, L. A. Taylor, E. Hill, and J. M. D. Day</i>	5207
Simulation of Nanophase Iron in Lunar Soil for Use in ISRU Studies <i>Y. Liu, L. A. Taylor, E. Hill, and J. M. D. Day</i>	5203

SHORT-LIVED NUCLIDES AND THE ORIGIN OF THE SOLAR SYSTEM. S. B. Jacobsen¹. ¹Department of Earth and Planetary Sciences, Harvard University, Cambridge, MA 02138, USA.

Introduction: A number of now extinct short-lived nuclides, with half-lives ranging from $\sim 10^5$ (^{41}Ca) to 10^8 years (^{146}Sm), were present in the early solar system and provide constraints on chronometry and nucleosynthetic sources of early solar system materials. Many different stellar sources have been suggested. Some nuclides (such as ^{26}Al , ^{41}Ca , ^{60}Fe) may be from contamination of the pre-solar molecular cloud by a single stellar source [supernova (SN), TP-AGB star or W-R star] close to the time of solar system origin. Other nuclides (such as ^{146}Sm , ^{244}Pu , ^{182}Hf and ^{129}I) may primarily reflect the average composition of the interstellar medium (ISM) at the origin of the solar system.

Model: The average ratio of a short-lived radioactive (R) isotope to a stable (S) reference isotope (N_R/N_S) in the ISM can be estimated from well established principles [1]. Normalizing this ratio to the nucleosynthetic production ratio (P_R/P_S), defines the parameter $\alpha_{R/S} = (N_R/N_S)/(P_R/P_S)$ which has a simple relationship to the mean life, τ_R , of R : $\log \alpha_{R/S} = \log \tau_R - \log T^*$ where $T^* = T \langle \psi \rangle / \psi(T)$, $\langle \psi \rangle$ is the mean nucleosynthetic production rate, T is the duration of nucleosynthesis, $\psi(T)$ is the final production rate and $\psi(t)$ is the time dependent mass production rate from stellar sources injected into the ISM. Thus, the average ISM values of the short-lived nuclides should lie on a line with a slope of 1 in a $\log \alpha_{R/S}$ vs. $\log \tau_R$ diagram. A new two-reservoir model for the ISM makes it possible to evaluate the short-lived nuclide pattern in terms of the residence time of matter in molecular clouds (MCs) [2]. For MCs we have the following relationship: $\log \alpha_{R/S} = 2 \log \tau_R - \log[(1 - x_{SI})\tau_{12} + \tau_R] - \log T^*$ where τ_{12} is the residence time of matter in MCs and x_{SI} is the mass fraction of matter in MCs (~ 0.2). For $\tau_{12} \gg \tau_R$, $\log[0.8\tau_{12} + \tau_R]$ is approximately constant and in this case the slope will be close to 2 for a MC.

Results and Conclusions: There are three groups of short-lived nuclides in a plot of $\log \alpha$ vs. $\log \tau$: (i) ^{53}Mn , ^{182}Hf , ^{244}Pu and ^{146}Sm lie on a trend with a slope somewhat less than 2, yielding a residence time of matter in MCs of $\tau_{12} \sim 6 \times 10^7$ yrs. These nuclides are likely produced by SNII sources injected into the interstellar medium over the history of our galaxy, (ii) ^{129}I and ^{107}Pd are substantially below this trend and likely produced by SNIa sources which appear to have been more common earlier in the history of our galaxy and (iii) ^{41}Ca , ^{26}Al and ^{60}Fe are too high to be of average galactic production; these must be a contamination from young stellar sources (dissimilar to typical SN sources) that formed within the proto-Solar MC. Thus, the pattern of short-lived nuclides is consistent with the birth of the solar system in a MC complex that was exchanging matter with (1) the remaining ISM at a timescale of $\sim 6 \times 10^7$ yrs and (2) with addition of fresh nucleosynthetic matter from young stars in this region at the time of solar system formation. The interpretation of the $\log \alpha$ - $\log \tau$ diagram by Cameron and Lodders [3,4] is incorrect.

References: [1] Schramm D. N. and Wasserburg G. J. 1970. *ApJ*. 162:57–69. [2] Jacobsen S. B. 2005. *ASP Conference Series* 30:. [3] Cameron A.G.W. and Lodders K. 2004. Abstract #1181. 35th Lunar and Planetary Science Conference. [4] Lodders K. and Cameron A.G.W. 2004. Abstract #1186. 35th Lunar and Planetary Science Conference.

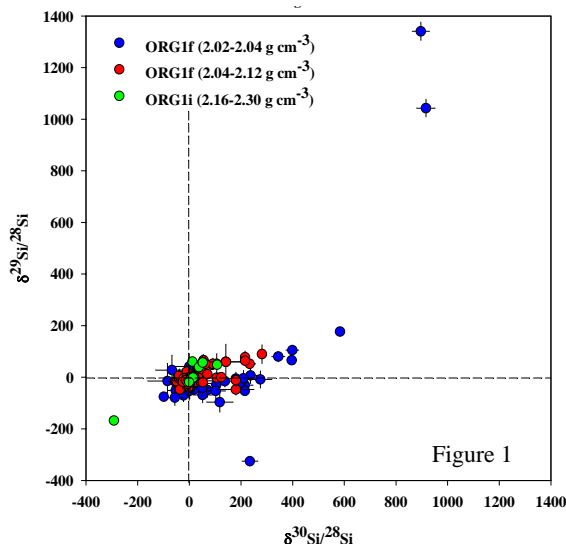
CONTINUED ISOTOPIC STUDIES OF PRESOLAR GRAPHITE FROM ORGUEIL.

M. Jadhav¹, S. Amari¹, E. Zinner¹, and T. Maruoka^{1*}, ¹Laboratory for Space Sciences, Washington University, St. Louis, MO 63130, USA. (mjadhav@wustl.edu)
*present address: Graduate School of Life and Environmental Sciences, University of Tsukuba, Ibaraki 305-8572, Japan.

Introduction: Earlier this year we reported the successful isolation of presolar graphite from Orgueil [1]. We presented NanoSIMS C and O isotopic data on three density fractions: ORG1b (1.59-1.67 g cm⁻³), ORG1d (1.75-1.92 g cm⁻³) and ORG1g (2.04-2.12 g cm⁻³). While only isotopically normal grains were found in ORG1b, ORG1d, and ORG1g have presolar graphite as indicated by their C isotopes. Ten grains from ORG1d have ¹⁸O excesses, indicating a supernova (SN) origin. Here we report C, N, O and Si isotopic analyses of three new density fractions: ORG1c (1.67-1.75 g cm⁻³), ORG1f (2.02-2.04 g cm⁻³) and ORG1i (2.16-2.30 g cm⁻³) and N and Si isotopic data on the anomalous fractions (ORG1d and ORG1g).

Experimental: Carbonaceous grains identified by X-ray analysis in the SEM were analyzed in the NanoSIMS in multidetection mode. ¹²C⁻, ¹³C⁻, ¹⁶O⁻ and ¹⁸O⁻ (phase 1) and, ¹²C¹⁴N⁻, ¹²C¹⁵N⁻, ²⁸Si⁻, ²⁹Si⁻ and ³⁰Si⁻ (phase 2) secondary ions were counted by bombarding the sample with a Cs⁺ primary beam.

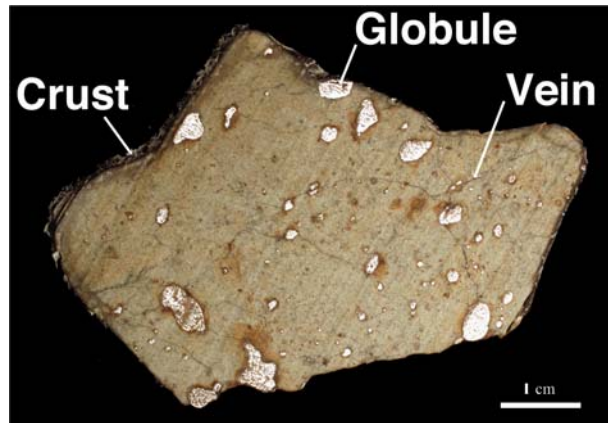
Results and Discussion: The new fractions, ORG1c, 1f and 1i all contain presolar graphite with ¹²C/¹³C ratios that range from 4-1746. The abundance of grains with isotopically light carbon increases with density. ORG1c has one ¹⁸O-rich grain but ORG1f and 1i exhibit solar ¹⁶O/¹⁸O ratios. This agrees with the trend reported previously in Orgueil and Murchison [1, 2], that the abundance of ¹⁸O-rich grains decreases with increasing density. Seven out of the ten ¹⁸O-rich grains from ORG1d were found to be enriched in ²⁸Si. Both these signatures point to a SN origin [3]. These grains also contain isotopically heavy nitrogen. The rest of the fractions have relatively normal ¹⁴N/¹⁵N ratios, with a few exceptions that are enriched in ¹⁵N. Figure 1 shows the ²⁹Si/²⁸Si and ³⁰Si/²⁸Si ratios measured in the heavy fractions ORG1f, 1g and 1i. While the lower-density fractions have ²⁸Si-rich grains, these high-density fractions have grains that are enriched in ³⁰Si and ²⁹Si. Most ³⁰Si-rich grains contain isotopically light carbon. These signatures are expected for low-metallicity AGB stars where ¹²C and ^{29,30}Si are dredged up from the He shell into their envelopes. These stars are the most likely source for the high density graphite grains in Orgueil that display ³⁰Si and ¹²C excesses.



References: [1] Jadhav M. et al. 2005. Abstract #1916. *LPS XXXVI*. [2] Hoppe P. et al. 1995. *GCA* 59: 4029-4056. [3] Travaglio C. et al. 1999. *ApJ*. 510, 325-354.

SAHARA 03500: A UNIQUE ACHONDRITE. Albert JAMBON¹ and Bertrand DEVOUARD^{2,3} ¹Laboratoire MAGIE, Université P. et M. Curie, Paris. ²UFR des Sciences de la Terre, Université P. et M. Curie, Paris. ³Laboratoire Magmas et Volcans, UMR 6524, Clermont-Ferrand, France. jambon@ccr.jussieu.fr

SAHARA 03500 collected in march 2003, is a single stone of 221 g. A nice greenish crust is preserved on one side. Centimetric to micrometric globules of sulfide and metal (about 6 vol. %) are dispersed in a light fine grained silicate matrix. A few fine dark shock veins crosscut the rock.



Mineralogy: The silicate matrix exhibits a magmatic texture with subhedral olivine (Fo70, 40 vol. %) and Pigeonite (En66-Fs30-Wo4, 25 %) rimmed by augite (En43-Fs22-Wo35, 13 %) surrounded by interstitial glass of nearly feldspathic composition (13%). The largest globules contain dendritic kamacite (2%) surrounded by pyrrhotite (4%). In smaller globules, sulfide is peripheral with metal exsolved as fine dendrites; a core of metal contains dominant kamacite with fine winding exsolutions of taenite and globular schreibersite. Some parts of the section appear severely brecciated..

Chemistry: Bulk chemical analysis indicate a nearly chondritic composition close to LL chondrites with significant differences though. The K/Na ratio is about 8 times CI. The REE pattern is slightly enriched in light REE while the heavy REE are flat. The Fe/Ni/Co ratios and abundances indicate clearly that the rock has lost a significant siderophile component.

Conclusions: SAH 03500 is a primitive achondrite marginally differentiated from a chondritic precursor.. It probably suffered significant impact melting and rapid cooling at the surface of a chondritic asteroid.

HETEROGENEOUS Th-U-Pb ISOTOPE AND ELEMENTAL SYSTEMATICS IN CALCIUM-ALUMINUM-RICH INCLUSIONS DETERMINED BY LA-ICPMS. K.P. Jochum¹, J.M. Friedrich², D.S. Ebel² and S.J.G. Galer¹. ¹Max-Planck-Institut für Chemie, Postfach 3060, 55020 Mainz, Germany (kpj@mpch-mainz.mpg.de; sjg@mpch-mainz.mpg.de). ²Department of Earth and Planetary Sciences, American Museum of Natural History, New York, NY 10024-5192, USA.(fried@amnh.org; debel@amnh.org).

Introduction: It is generally believed that Ca, Al-rich inclusions (CAIs) formed in the solar nebula very early by high temperature processes. Lead isotopes can provide absolute formation ages of CAIs with high precision [1,2]. The most precise ages of 4566 ± 2 Ma [3] and 4567.2 ± 0.6 Ma [4] have been determined for CAIs from the CV chondrites Allende and Efremovka, respectively. Lead isotopes also contain a record of the chemical environment in which the Pb resided via their uranium and thorogenic Pb components. There are only a few investigations of Th-U-Pb systematics in CAIs, and none with high spatial resolution. To obtain further insight, we used LA-ICPMS to determine ²⁰⁸Pb/²⁰⁶Pb, ²⁰⁷Pb/²⁰⁶Pb ratios, and Pb, Th, U abundances in CAIs and matrix from the carbonaceous chondrites Allende, Axtell, Vigarano, Gao Guenie (b), Leoville and NWA-2364.

Experimental: Analyses were done with a New Wave UP 213 Nd:YAG laser ablation system combined with a single-collector sector-field ThermoFinnigan ELEMENT2 ICPMS [5]. To measure the Pb, Th and U isotopes as precisely as possible, the fast electrical mode was used. Point analyses were done using laser spot diameters of 80 – 120 μm at an energy density of about 7 J/cm². Ablation times were about 60 – 80 s, with a few μg sample being ablated per analysis. Typically, a single spot analysis consisted of about 150 blank and 500 ablation measurements. Mass fractionation was calibrated using intercalated measurements of the MPI-DING KL2-G reference glass [5]. We obtained in-run precisions (1 RSE) of about 0.2 – 0.5 % on ²⁰⁷Pb/²⁰⁶Pb and ²⁰⁸Pb/²⁰⁶Pb for concentrations of 2 to 0.2 ppm. Unfortunately, ²⁰⁴Pb cannot be reliably determined at this level. Th/U and Pb/U elemental ratios could be measured with a precision of about 1 %.

Results and discussion: The Pb isotopic compositions of the matrix (²⁰⁸Pb/²⁰⁶Pb = 3.1, ²⁰⁷Pb/²⁰⁶Pb = 1.1) from the various chondrites are almost primordial [6]. In contrast, 175 CAI measurements show extremely variable Pb isotope ratios: ²⁰⁷Pb/²⁰⁶Pb and ²⁰⁸Pb/²⁰⁶Pb ratios range from about 1 to 0.63, and 0.6 to 4.1, respectively. Measured Pb/U and Th/U ratios are also quite variable. For example, Th/U ratios in Allende CAIs vary from about 3 to 15 whereas the matrix value is 3.75 ± 0.11. Assuming a single-stage model and an age of CAIs of 4560 Ma, the μ (²³⁸U/²⁰⁴Pb) and κ (²³²Th/²³⁸U) values lie between about 2 - 300, and 3 - 18, respectively. Similarly, measured versus calculated U/Pb and Th/U ratios are well correlated for the individual CAI spot analyses, showing that the Th-U-Pb system has not been significantly disturbed at the ~100 μm scale.

References: [1] Chen J.H. and Wasserburg G.J. 1981. *Earth Planet. Sci. Lett.* 52:1-15. [2] Manhès G. et al. 1987. *Meteoritics* 22:453-454. [3] Allègre C.J. et al. 1995. *Geochim. Cosmochim. Acta* 59:1445. [4] Amelin Y. et al. 2002. *Science* 297:1678-1683. [5] Jochum K.P. et al. 2005. *Int. J. Mass Spectr.* 242:281-289. [6] Tatsumoto M. et al. 1973. *Science* 180:1279-1283.

SYNTHESIZING ORGANICS USING AMORPHOUS Mg- AND Fe- SILICATE GRAINS

N. M. Johnson^{1,2}, M. Martin³, J. P. Dworkin¹, and J. A. Nuth III¹. ¹Astrochemistry Lab, NASA's Goddard Space Flight Center, Greenbelt, MD. ²NAS/NRC Resident Research Associate. ³The Catholic University of America, Washington, DC.

Introduction: It is unknown what exact process or combination of processes produced organics that are found in meteorites or are detected in comets and nebulas. One particular process that forms organics are Fischer-Tropsch type (FTT) reactions. Fischer-Tropsch type synthesis produces complex hydrocarbons by hydrogenating carbon monoxide via surface mediated reactions. The products of these reactions have been well-studied using 'natural' catalysts [1] and calculations of the efficiency of FTT synthesis in the Solar Nebula suggest that these types of reactions could make significant contributions to the composition of material near three AU [2]. We use FTT synthesis to coat Fe-silicate and Mg-silicate amorphous grains with organic material to simulate the chemistry in the early Solar Nebula. These coatings were found to be composed of macromolecular organic phases [3]. Previous work also showed that as the grains became coated, Haber-Bosch type reactions took place resulting in nitrogen-bearing organics [4].

We discuss the differences/similarities of the produced organics (solid and gas phase) and their production rates using either amorphous Mg- silicate grains or amorphous Fe- silicate grains as the starting material.

Experiments: We circulate CO, N₂, and H₂ gas through Fe- or Mg- amorphous silicate grains that are maintained at a specific temperature. The gases are passed through an FTIR spectrometer and are measured to monitor the reaction progress. Each cycle begins with 75 torr N₂, 75 torr CO, and 550 torr H₂ before the grains are brought to temperature (i.e., 400 or 500°C). After the gas has circulated for a predetermined amount of time, the heating element is turned off and the gas is pumped away. We repeat this process approximately fifteen times.

In addition to real time gas measurements using FTIR, we periodically collect a gas sample for additional analysis using a cold trap and a solvent (e.g., high purity acetonitrile). We analyze the 'trapped' gas sample using GCMS. Solid samples are analyzed using FTIR, GCMS (including pyrolysis) and potentially by NMR spectroscopy. Extraction techniques are also used to analyze the organic coatings.

Discussion: These experiments show that these types of reactions are an effective process to produce complex hydrocarbons. In the future, we will subject the reacted samples to thermal annealing and/or hydration to determine how these processes affect the deposited organic layers. These secondary processes would mimic what may have occurred on meteorite parent bodies and ideally give insight into the history of meteoritic organics. Overall, organics generated in this manner could represent the carbonaceous material incorporated in comets and meteorites.

References: [1] Hayatsu R. and Anders E. 1981. *Topics in Current Chemistry* 99:1-37. [2] Kress M. E. and Tielens A. G. G. M. 2001. *Meteoritics & Planetary Science* 36:75-91. [3] Johnson N. M. et al. 2004. Abstract #1876. 35th Lunar & Planetary Science Conference. [4] Hill H. G. M and Nuth J. A. 2003. *Astrobiology* 3:291-304.

SOUTH POLE-AITKEN BASIN AND THE COMPOSITION OF THE LUNAR CRUST. B. L. Jolliff¹ and J. J. Gillis².

¹Dept. of Earth and Planetary Sciences, Washington University, St. Louis. E-mail: blj@wustl.edu. ²Hawaii Inst. of Geophysics and Planetology, U. Hawaii.

The early differentiation of the Moon generated a crust strongly enriched in alumina as well as trace elements that are incompatible in basaltic systems. Knowledge of rocks and soils from the lunar surface, coupled with global compositional remote sensing, allow us to infer the composition of the crust. The weakest link in understanding the bulk crustal composition is the deep crust, which also holds key information about the nature of the crust-mantle separation during magma-ocean solidification. South Pole-Aitken basin (SPA) excavated deep into the crust and, despite an extensive history of post-SPA impacts, the materials remaining in and around the SPA basin retain a record of the deep crustal composition (see below). This composition can be used to address key questions such as: (1) is the deep crust heterogeneous in different regions of the Moon, as is the case for the major surface compositional "terranes," (2) is KREEP uniformly distributed in the lower crust, and (3) is the lower crust significantly more mafic than the upper crust and is it ferroan or magnesian?

Thorium and Fe concentrations, which were well determined by the Lunar Prospector gamma-ray spectrometer (LPGRS), have been binned to half-degree per pixel resolution [1] and have been correlated and validated empirically using sample-based data sets [2]. Either of these two elements projected globally show clearly the compositional anomaly of the SPA basin. The basin has elevated Fe relative to its surroundings, with FeO typically in the range of ~8-11 wt.%. This enrichment occurs across the entire basin and is not localized near small exposures of mare basalts. Thorium concentrations are also elevated relative to surroundings, ranging 1-4 ppm, with a mean of ~2 ppm. For comparison, the surrounding feldspathic highlands range 0-3, with a mean of ~0.5 ppm. On the other side of the planet, the Procellarum KREEP Terrane (PKT) exposes materials with Th concentrations ranging to >12 ppm. If the latter concentrations reflect KREEP-bearing materials derived from the lower crust, then the SPA basin, which excavated deep-seated materials, did not sample similarly KREEP-enriched lower-crustal material. Mass-balance calculations for Th suggest that the PKT is the anomalous region and that the SPA basin exposed more typical lower crust. Taking the SPA basin as representing the lower part of a layered crust leads to whole-Moon Th concentrations of roughly 2-3×chondritic, depending on crustal thickness and on whether the mantle is differentiated throughout its depth.

Concentrations of Mg determined by the LPGRS are available only for 5-degree resolution. Using data released June 2002, values of $Mg/(Mg+Fe) \times 100$ range mainly 64-72, with a mean of 68, which is modestly ferroan. At issue is whether the lower crust is a ferroan complement to the anorthositic upper crust. However, without better knowledge of the mix of lower crust, upper mantle, and mare basalt (including cryptomare) in SPA regolith, this remains an open question. Data from the SMART-1 X-ray spectrometer may improve these values.

References: [1] Lawrence D.J. et al., 2003, *Lunar Planet. Sci.* 34, Abstract #1679; [2] Gillis, J.J. et al., 2004, *Geochim. Cosmochim. Acta* 68, 3791-3805.

CALCULATIONS OF LUNAR BULK COMPOSITION.

J. H. Jones, KR, NASA/JSC, Houston, TX 77058.
(jjones2@em.s.jsc.nasa.gov)

The bulk composition of the Moon is of considerable interest. Quite probably, if we knew the Moon's composition, we would have a much better understanding of the Moon's origin than we currently do. Therefore, it is important to understand how estimates of the Moon's composition are derived and the assumptions that are required in these calculations. As will be seen below, very small differences in the boundary conditions of a bulk composition calculation can lead to important difference in the results. Of course, the real reason for these differences and uncertainties is because we have no sample of undifferentiated lunar matter. Unlike the Earth, where we believe we can sample nearly undifferentiated bulk silicate Earth (BSE) as mantle xenoliths, there are no samples of the bulk silicate Moon (BSM). Nor are there lunar basalts that are unequivocally from undifferentiated source regions. Consequently, we resort to calculation.

There are two main classes of calculated BSM — "Earth-like" and "refractory enriched." The Earth-like category has been advocated by Wänke and co-workers, Ringwood and co-workers, and Jones and Delano, and I will rely heavily on the Jones and Delano discussion here. In the models derived by these researchers, the Moon is viewed as generally chondritic and Earthlike in its refractory elements (CaO, MgO, and Al₂O₃), differing from the Earth mainly by enrichment in FeO and depletion in volatile elements like Na and K.

The refractory-enriched Moon has been championed by Taylor and co-workers and by some geophysical studies. In these models the Moon has ~1.5X the CaO and Al₂O₃ of the Earth. Enrichment of these refractory oxides is often ascribed to depletion of less refractory elements such as MgO and SiO₂, which are believed to have been lost by volatilization during a giant impact event.

All models of lunar composition must make some assumption about the value of a major element ratio such as Mg/Si or Mg/Al. Taylor assumed that the Moon possessed a CI Mg/Si ratio (0.93). Conversely, Wänke and Ringwood, believing that the Earth and Moon were formed from similar materials at the same heliocentric distance, used a terrestrial Mg/Si ratio (~1.1). Jones and Delano, believing on theoretical grounds that Si might be more volatile than Mg or Al, chose to use a CI Mg/Al ratio.

With hindsight, it turns out that the choice of major element ratio that was used in BSM calculation determines whether the result is Earth-like or refractory enriched. The Wänke-Ringwood Moon is not refractory enriched because the higher Mg/Si ratio requires that there be ~30% more normative olivine, which dilutes the refractory component. Ironically, the choice of a CI Mg/Al in the Jones and Delano calculation produced almost exactly the same result as choosing a terrestrial Mg/Si ratio.

STUDIES OF ^{14}C AND ^{10}Be PRODUCTION RATES AND TERRESTRIAL AGES OF DESERT METEORITES. A. J. T. Jull¹, L. R. McHargue¹, K. J. Kim¹, J. A. Johnson¹, P. A. Bland² & A. W. R. Bevan³. ¹NSF Arizona AMS Laboratory, University of Arizona, Tucson, AZ 85721, USA. E-mail: jull@email.arizona.edu ²Department of Geology, Imperial College, London SW7, UK. ³Western Australian Museum, Francis St., Perth, WA 6000, Australia.

Introduction: We have investigated the terrestrial ages, or residence time on the Earth's surface, of 76 meteorites from Western Australia, and one from South Australia, using both ^{14}C measurements and also $^{14}\text{C}/^{10}\text{Be}$. Some of the ^{14}C measurements have been reported previously [1]. We have now included ^{10}Be measurements from 30 meteorites. We find that the $^{14}\text{C}/^{10}\text{Be}$ terrestrial ages are more precise than ^{14}C alone, since we can correct for shielding effects. We compared the two different age determinations, where measured, which generally agreed within 1-2ka.

Production rates: Kring et al. [2] and Welten et al. [3,4] assumed a constant production ratio of ^{14}C to ^{10}Be , in order to use ^{10}Be as a shielding correction for ^{14}C terrestrial ages of meteorites of 2.5 to 2.6. In general, ordinary chondrites all have saturated ^{10}Be (exposure ages $>5\text{Myr}$) and any low value of ^{10}Be is due to shielding [5]. For meteorites of lower exposure age, it is important to correct for the exposure age. We have modeled the behavior of $^{14}\text{C}/^{10}\text{Be}$ vs. ^{10}Be for different-sized meteoroids. Our results indicate that for meteoroids of radius (R) $>30\text{cm}$, $^{14}\text{C}/^{10}\text{Be}$ increases with depth into the object. For larger objects, $R>50\text{cm}$, $^{14}\text{C}/^{10}\text{Be}$ is highest close to the center, 2.5 to 3.0 and declines to ~ 2.0 at the surface of these objects. For smaller objects, $R<25\text{cm}$, $^{14}\text{C}/^{10}\text{Be}$ ratios are 2.0 or less.

Experimental: We have compared the modeling to ^{14}C and ^{10}Be results from known falls and to 12 Western Australian (WA) meteorites of low terrestrial age ($T_{\text{terr}}<2\text{kyr}$). An intriguing result is that we found that these WA meteorites studied must have come from object with $R>45\text{cm}$. We also found one meteorite (Mundrabilla 005) which has an unusually high value of $^{14}\text{C}/^{10}\text{Be}$.

Summary: In principle, improved precision on ^{14}C terrestrial ages can be achieved by using $^{14}\text{C}/^{10}\text{Be}$ to correct for shielding [2,3,4], or using $^{22}\text{Ne}/^{21}\text{Ne}$ as noted by Schultz et al. [6]. However, it is clear a better understanding of the systematics of changes of these various nuclides as a function of depth in the meteoroid must also be taken into account.

References: [1] Bland P. A. et al. 2000. *Quaternary Research* 53:131. [2] Kring D. A. et al. 2001. *Meteoritics and Planetary Science* 36:1057. [3] Welten K. C. et al. 2001. *Meteoritics and Planetary Science* 36: 201. [4] Welten K. C. et al. 2004. *Meteoritics and Planetary Science* 39: 481. [5] Graf Th. et al. 1990. *Geochimica et Cosmochimica Acta* 54: 2521. [6] Schultz L. et al. 2005. *Meteoritics and Planetary Science* 40, in press.

SPECTRUM IMAGING OF SPACE-WEATHERED RIMS ON LUNAR SOIL GRAINS. L. P. Keller¹ and R. Christoffersen².

¹Mail Code KR, NASA Johnson Space Center, Houston, TX 77058, ²SAIC, 2200 Spacepark Dr., Houston, TX 77058.

Introduction: Space weathering processes modify the structure, composition and optical properties of materials exposed at the lunar surface. These processes obscure the characteristic absorption bands used in remote sensing to infer the mineralogy and composition of lunar regions [e.g. 1, 2]. Lunar soil grains exhibit a range of effects in response to space weathering including erosion and amorphization from solar wind irradiation, and accumulation of impact generated vapors and sputtered species [3]. Soil grains with complex layered rims record multiple events of irradiation and vapor deposition [3], while ion-mixing and radiation-enhanced diffusion effects can further obscure the relative contributions of irradiation and condensation to rim formation [4]. With recent advances in instrumentation [5], we are gaining new insights into space weathering effects through quantitative nm-scale chemical mapping of grain rims.

Samples: We used a JEOL 2500SE 200 keV field-emission scanning-transmission electron microscope (TEM) equipped with a thin window energy-dispersive X-ray (EDX) spectrometer to obtain spectrum images of several grain rims in ultramicrotome thin sections (~50 nm thick) of an aliquot of Apollo 11 soil 10084 (sub-20 μm sieve fraction). Each pixel of a spectrum image contains a full EDX spectrum, enabling the determination of quantitative element abundances on the scale of individual pixels. Spectrum images of the lunar grains were acquired with a 4 nm incident probe whose dwell time was minimized to avoid beam damage and element diffusion during mapping. Successive image layers of each rim were acquired and combined in order to achieve suitable counting statistics for major elements (e.g. Mg, Al, Si, Ca, Ti, and Fe) in each pixel.

Results and Discussion: We mapped the elemental distributions in rims on grains of cristobalite, anorthite, ilmenite and glass. An amorphous (irradiated) rim on cristobalite showed no discernable chemical effects. Spectrum images of inclusion-rich (deposited) rims on anorthite reveal that the rims are compositionally heterogeneous at the sub- μm scale around the circumference of the grains – the differences are particularly noticeable in the Mg, Fe, Ti maps, reflecting episodic deposition. EDX mapping also has revealed internal stratigraphy within the thickness of a rim that is also consistent with multiple deposition events (>3). Ilmenite rims show complex zoning patterns from the combination of vapor deposition and radiation effects. We confirm earlier work [3] showing the preferential loss of Fe from the surfaces of the ilmenite, segregation of Fe into nanophase Fe metal grains, and the formation of a Ti-rich surface layer. Silicate material has been deposited on the ilmenite grains – as discrete thin layers, but in one grain as a diffuse layer that is suggestive of extensive ion-mixing between the silicate material and host ilmenite.

Conclusions: Spectrum imaging of space weathered rims on lunar soil grains reveals new complexities about their formation, including the number of events and range of processes that are involved.

References: [1] Pieters, C. M. *et al.* (2000) *MPS*, 35, 1101. [2] Noble, S. K. *et al.* (2001) *MPS*, 36, 31. [3] Keller, L. P. and McKay, D. S. (1997) *GCA* 61, 2331. [4] Christoffersen, R. *et al.* (1996) *MPS*, 31, 835. [5] Keller, L. P. (2005) *Microscopy & Microanalysis*, in press.

QUANTITATIVE REANALYSIS OF NEAR-INFRARED SPECTROSCOPIC DATA FOR ASTEROID 4953 1990 MU.
M. S. Kelley¹ and M. J. Gaffey². ¹Department of Geology and Geography, Georgia Southern University, Statesboro, GA 30460-8149. E-mail: mkelley@georgiasouthern.edu. ²Department of Space Studies, University of North Dakota, Grand Forks, ND 58202-9008.

Asteroid 4953 1990MU was observed over the 0.8-2.5 μm spectral interval using the 52-channel double CVF system at the NASA Infrared Telescope Facility. Preliminary analysis of these data [1] reported a compositional heterogeneity over the surface of this asteroid. A careful reanalysis of the dataset has resulted in a better understanding of the spectral characteristics of 4953, and quantitative analysis of the near-infrared absorption band parameters has been performed following procedures described by [2]. This latest work supports the previous interpretation of body with at least two distinct mineralogical regions on its surface.

The near-infrared spectrum from 4 June 1994 exhibits a significant, well-defined absorption feature near 1.2-1.3 μm . There are three possible explanations for this feature: (1) it is due to the presence of a large feldspar component on the asteroid; (2) it is a side lobe of an olivine absorption feature; (3) it is due to the presence of a high-Fe pyroxene component. If this feature is feldspathic, it would rule out a chondritic nature for the asteroid.

Lightcurve segments were extracted from infrared data collected on two consecutive nights. Based on these segments, it was previously reported [1] that the most likely rotation period appeared to be 6.5 hours. Subsequent work by [3] used discreet filter data to obtain a lightcurve with a period of 14.218 hours. A smaller dataset for two nights by Erikson *et al.* (2000) includes only one lightcurve minimum and one maximum, but appears to be consistent with the lightcurve of Mottola *et al.*

References: [1] M. S. Kelley and M. J. Gaffey 1995, 26th Lunar and Planetary Science Conference, p. 731. [2] M. J. Gaffey *et al.* 2003, In Asteroids III, pp. 183-204. [3] S. Mottola *et al.* 1995, *Icarus* 117, 62-70. [4] A. Erikson *et al.* 2000. *Icarus* 147, 487-497.

GEOCHEMISTRY, MINERALOGY, AND WEATHERING OF THE ANTARCTIC FERRAR DOLERITE WITH IMPLICATIONS FOR MARTIAN METEORITES AND SURFACE PROCESSES J. D. Kennedy¹ and R. P. Harvey¹.

¹Dept. of Geological Sciences, Case Western Reserve University, Cleveland OH 44106-7216. E-mail: jdk40@case.edu

Introduction: Samples of the Antarctic Ferrar Dolerite are an excellent analog to Martian igneous lithologies on a variety of scales. In thin section, they show mineralogical and geochemical similarities to the Martian SNC meteorites [1]. On the outcrop scale, they display similar weathering features observed in rocks at numerous Viking [2], Pathfinder [3], and MER [4] mission sites. Here, we present preliminary mineralogical analyses from relatively fresh (unexposed) dolerite samples, with comparisons to SNC meteorites and weathered Antarctic dolerites.

Mineralogy: Thin sections from a comparatively unweathered Ferrar dolerite sample were analyzed using scanning electron microscopy. Quantitative results from elemental X-ray map spectra confirm the presence of at least two pyroxenes (augite and pigeonite), two feldspars, and Fe- and Ti-oxides. The dolerite pyroxene assemblage is a very good match to Shergottite pyroxenes in terms of both range and average. The feldspar assemblage is also quite similar, though presently we have less data from these. The modal abundance of pyroxenes and feldspars in the Ferrar dolerite differs from that of the Shergottites; feldspar is more abundant than pyroxene in the former, while the reverse is generally true in the shergottites.

Backscatter electron images from Ferrar thin sections reveal subhedral pyroxene and feldspar crystals, with the pyroxenes showing a range of zoning styles and fracturing. Most of these crystals display normal zoning (Mg-rich cores with Fe-rich rims), while the remainder show more complex and intricate zoning. Pigeonite overgrowths are common on larger augite crystals. Many of these features are commonly observed in the SNC meteorites [5, 6].

Weathering: Augite in weathered Antarctic dolerite samples appears deficient in FeO compared to unweathered samples. Augite from weathered samples [7] cluster around $^{30}\text{Wo}^{56}\text{En}^{14}\text{Fs}$ [7] while those from unexposed samples form a typical igneous fractionation trend, ranging from about $^{30}\text{Wo}^{40}\text{En}^{30}\text{Fs}$ to $^{30}\text{Wo}^{25}\text{En}^{45}\text{Fs}$. The likely cause of this FeO deficiency is oxidation to Fe_2O_3 , resulting in the prevalent green-to-red color transition observed between fresh and more weathered samples. Further study will investigate this Fe loss in detail using Mössbauer spectroscopy and thorough electron microprobe analysis. Direct comparison of future data with results from the MER rovers' Mössbauer spectrometers should lead to a better understanding of dynamic geochemical and geomorphologic processes that have occurred, and might still be present, on Mars.

References: [1] Harvey R.P. 2001. Field Trip and Workshop on the Martian Highlands and Mojave Desert Analogs, LPI Contribution 1101, 25. [2] Allen C.C. and Conca J.L. 1991. *Proceedings of Lunar and Planetary Science* 21:711-717. [3] Rodriguez-Navarro C. 1998. *Geophysical Research Letters* 25:3249-3252. [4] Rice J.W. 2004. *Abstracts with Programs – Geological Society of America* Vol. 36, no. 5, p. 21. [5] Harvey R.P. and McSween H.Y. 1991. *Geochimica et Cosmochimica* 56:1655-1663. [6] McSween H.Y. and Treiman A.H. 1998. in *Reviews in Mineralogy* 36:6.1-6.53 [7] Talkington R.W. et al. 1982. *Geological Magazine* 119:553-566.

THE EFFECTS OF GEOMETRY ON NUCLIDE PRODUCTION PROCESSES IN METEORITES.

K. J. Kim^{1,2}, J. Masarik³, and R. C. Reedy¹ ¹Inst. of Meteoritics, Univ. New Mexico, Albuquerque, NM 87131 USA. ²Present address: Lunar & Planetary Lab., Univ. Arizona, Tucson, AZ 85721 USA E-mail: kkim@lpl.arizona.edu ³Dept. Nuclear Physics, Komensky University, SK-842 15 Bratislava, Slovakia.

Introduction: The rates for making cosmic-ray-produced (“cosmogenic”) nuclides in meteorites are often assumed to only vary with the mass or volume of the pre-atmospheric body (the meteoroid) and abundances of the target elements. As discussed in [1], bulk composition affects production rates. A meteoroid’s shape can also affect production rates [e.g., 2] and cause the sizes of recovered superbolides as determined from cosmogenic nuclides to be different from those inferred from fireball measurements [e.g., 3]. From observations of asteroids, non-spherical shapes are probably the rule and spherical shapes the exception for small bodies in the inner solar system.

Production Rate Calculations: We adopted the L/LL-chondrite Knyahinya as the test case. Its pre-atmospheric radius was about 45 cm [4], and many cosmogenic nuclides have been measured at known depths [4,5]. It was often used as a test case for production-rate calculations with the codes used for our calculations, LCS [5] and MCNPX [6]. The bulk density was the recently measured value of 3.35 g/cm³ [7], less than the previously assumed 3.55 g/cm³, but it is not a critical parameter.

An L-chondrite composition was used [5,6]. The geometries were spheres of radii 25, 35, 45, and 55 cm and ellipsoids with the same volume as a 45 cm sphere but with one axis either twice as long or half as long as the other 2 axes.

Results: The production rates calculated for the spheres have the same trends previously reported by us and others, of increasing from the surface to the center with the amount of the increase and differences among radii being a function of the cosmogenic nuclide. Production rates for the ellipsoids were lower than those for a 45 cm sphere, with the cigar shape having slightly higher rates than the pancake one. The differences between the ellipsoids and 45 cm sphere varied with the nuclide.

Discussion: The shape of a meteoroid affects the rates for producing cosmogenic nuclides. Ellipsoids have lower production rates than a sphere of the same volume. This probably is mainly a consequence of there being shorter distances to a surface in ellipsoids than in a sphere, and thus rates in ellipsoids are like those for a sphere with a smaller volume. The shortest axis is an important parameter. Probably most radii inferred for meteoroids using cosmogenic nuclides assuming a spherical shape have volumes less than the meteoroid’s actual volume.

Acknowledgments: This work was supported by NASA’s Cosmochemistry Program and the Slovak Grant Agency VEGA.

References: [1] Masarik J. and Reedy R. C. 1994. *Geochim. Cosmochim. Acta* 58: 5307-5317. [2] Masarik J. and Reedy R. C. 1994. *Lunar Planet. Sci.* 25: 843-844. [3] Graf Th. et al. 1997. *Meteorit. Planet. Sci.* 32: 25-30. [4] Graf Th. et al. 1990. *Geochim. Cosmochim. Acta* 54: 2511-2520. [5] Reedy R. C. et al. 1993. *Lunar Planet. Sci.* 24: 1195-1196. [6] Kim K. J. and Reedy R. C. 2004. *Lunar Planet. Sci.* 35: #1359. [7] Britt D. T. and Consolmagno G. J. 2003. *Meteorit. Planet. Sci.* 38: 1161-1180.

THE STRATIGRAPHIC AND HISTORIC RECORD OF METEORITIC IMPACT EVENTS IN ALABAMA. D. T. King, Jr.¹ and L. W. Petruny². ¹Dept. Geology, Auburn U., AL 36849 USA [kingdat@auburn.edu]. ²AstraTerra Research, Auburn AL 36831-3323 USA.

Commencing with the Wetumpka impact event ~83 m.y. ago and continuing to present, Alabama has had its fair share of meteoritic impact events, both large and small. Alabama's "heavy bombardment" era occurred during Cretaceous. Cosmic impact at Wetumpka (Elmore County) concerned a ~350-m diameter chondritic (?) asteroid, which struck in ~50 m of sea water covering the Mooreville shelf [1]. Both crystalline bedrock and overlying Upper Cretaceous sediments were involved in local deformation during this impact, which is marked by a deeply eroded, 7.6-km diameter, semi-circular rimmed impact structure. Effects of the 65-Ma Chicxulub (KT) impact event (~1250 km across the Gulf of Mexico) are well recorded in western Alabama's stratigraphic record where KT boundary tsunami sands (basal Clayton Formation) are deposited upon scoured and fractured late Maastrichtian marls [2, 3]. Alabama's "light bombardment" era of historic impacts was ushered in by the great Leonid meteor shower of November 12-13, 1833. Carl Carmer's 1934 book *Stars Fell on Alabama* recounts how this meteor shower was so spectacular in



Alabama's skies that – even a century afterward – ‘memories of the oldest ones’ marked time from “the year the stars fell.” This phrase found its way into popular song and now adorns Alabama's current automobile license tags. The historic era commences in earnest in late 1868 when two bolides, one over (Morgan County (on November 27) and the other over Franklin County (on December 5) were seen and the respective fallen bodies recovered. In 1900, a fiery bolide was seen and a fallen mass

recovered in Perry County (May 15). In 1907, a bright bolide was seen over Colbert County (January 12) and the fall recovered. The 1933 Athens bolide fell in Limestone County (July 11). The 1954 Sylacauga bolide (Talladega County, November 30) is celebrated for the stone having penetrated a house roof and causing a human injury. On December 5, 1999, the Trans-Alabama superbolide illuminated almost all of Alabama and parts of four adjacent states as it crossed the state on a fiery southeasterly trajectory [4]. This potentially large meteoritic mass has not been recovered. It is interesting to note that 4 of the 7 Alabama historic bolide events occurred within 8 calendar days of one another (November 27-December 5), and two on the same day (December 5, 1868 and 1999)!

References: [1] King Jr. et al. 2002. *Earth and Planet. Sci. Let.* 202:541-549. [2] Smit J. et al. 1996. *Geol. Soc. Amer. Spec. Publ.* 307:151-182. [3] King Jr. D.T. and Petruny L.W. 2005. *Gulf Coast Trans. Geol. Soc.* 55. [4] King Jr. D.T. and Petruny L.W. 2003. *Eos, Trans. Amer. Geophys. Union* 84:253, 257.

TARGET-AFFECTED MORPHOLOGY OF THE WETUMPKA (MARINE) IMPACT CRATER, USA.

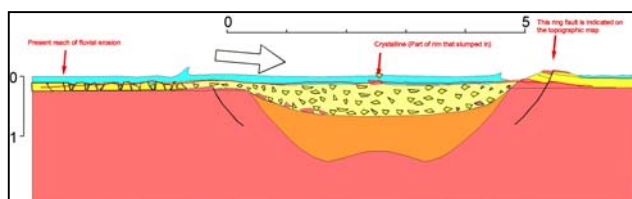
D.T. King, Jr.¹, J. Ormö², L.W. Petruny³, J.R. Morrow⁴, R.C. Johnson⁵, and T.L. Neathery⁶. ¹Dept. Geology, Auburn U., AL 36849 [kingdat@auburn.edu]; ²Centro de Astrobiología (INTA/CSIC), Madrid, Spain; ³AstraTerra Research, Auburn, AL 36831-3323; ⁴Dept. Earth Sci., Campus Box 100, Univ. Northern Colorado, Greeley, CO 80639; ⁵Dept. Geology, Auburn U., AL 36849; ⁶1212-H Veteran's Parkway, Tuscaloosa, AL 35404

Introduction: The Late Cretaceous Wetumpka marine-target impact structure is situated in the inner Coastal Plain of Alabama [1, 2]. The ~5-km structure is characterized by (1) a wide, horseshoe-shaped crystalline rim that is open on the SW quadrant, (2) an interior region of broken and disturbed sedimentary formations, and (3) an extra-crater terrain on the south-west composed of structurally disturbed target formations [2].

To understand the influence of target properties on the cratering and modification of Wetumpka, we examined its present state of preservation (i.e., the erosional level v. an original crater cross section). This was achieved by comparing present geology and topography with standard parameters for impact craters, but also incorporating observations from simulation studies of marine-target impacts [3], especially those strongly affected by the collapse of a thick sequence of poorly consolidated sediments (e.g., Chesapeake Bay [4]).

Target materials: In reverse stratigraphic order, the target consisted of (1) marine water (which was approximately 30-100 m deep and likely shallowed toward the north where the coeval shoreline was located); (2) poorly consolidated sediment (comprising 30 m of chalky ooze, (3) 30 m of paralic marine sand, and (4) 60 m of terrestrial clayey sand and gravels, and ultimately, weathered crystalline basement.

Cross-section: In this hypothetical cross-section, the parautochthonous breccia lens (orange) is formed by initial collapse of the transient cavity. Overlying slump deposits of sediments from the collapsing rim segment are marked with fragment symbols.



The crystalline basement has a SE dip of ~10 m/km, and this is assumed to play an important role in both cratering and later modification. In fact, selective failure of the SW rim is probably due to deeper target water and dip-related instability in that area and the resurge flow that caused failure of poorly consolidated sediments in that part of the rim. Via this process, Wetumpka's distinctive horseshoe-shape was formed.

References: [1] Neathery T.L. et al. 1976. *Geol. Soc. Amer. Bull.* 87:567-573. [2] King Jr. D.T. et al. 2002. *Earth and Planet. Sci. Letters* 202:541-549. [3] Ormö J. et al 2002. *Jour. Geophys. Res.* 107:E11. [4] Collins G.S. and Wünnemann K. 2005. Abst. #1736. 36th Lunar & Planet. Sci. Conf.

EARLY SOLAR SYSTEM GRANITES. P. L. King^{1,2}, K. N. Dalby¹, S. D. J. Russell¹, T. Ireland³, H. Y. McSween Jr.² and A. Bischoff⁴. ¹Dept. Earth Sciences, Univ. Western Ont., London ON N6A 5B7 Canada. penny.king@uwo.ca. ²Dept Earth Planet. Sci., Univ. Tennessee, Knoxville TN 37996 USA. ³Res. Sch. Earth Sci., Aust. Nat. Univ., Canberra ACT 0200 Australia. ⁴Inst. Planet., Wilhelm-Klemm-Str. 10, 48149 Münster, Germany.

Introduction: Granitic rocks (quartz, plagioclase + K-feldspar) are abundant in the Earth's continental crust, but are rare on other planetary bodies. We examined LL meteorites with granitic clasts or glasses (Adzhi-Bogdo and Vishnupur, [1]).

Granitic fragments in Adzhi-Bogdo: The Adzhi-Bogdo (LL3-6 breccia) contains mm-size granitic clasts, including one with zircon, tridymite, K-feldspar, and ilmenite, near clasts that also have albite, pyroxene, phosphates [2] and aenigmatite [3]. We analyzed U-Th-Pb isotopes in the zircon using the SHRIMP-RG at the ANU. Because the zircon was small (~15 μm long, <30 μm thick) only three full measurement cycles were possible with a 10 μm diameter O⁻ beam. The zircon had a ²⁰⁷Pb-²⁰⁶Pb age of 4.6 ± 0.2 Ga, plotting above concordia.

Granitic glasses in Vishnupur: The Vishnupur (LL-6) meteorite [4] contains μm -size glasses with granitic CIPW norms. We found that these glasses plot on the Ab-Or thermal divide (~1075-1300 °C) on a SiO₂-KAlSiO₄-NaAlSiO₄ diagram; similar to terrestrial syenites and high pressure glass inclusions from mantle-derived crystals [5]. The melt compositions are inconsistent with fractional crystallization, immiscibility, minimum-temperature melting or vapor-exchange; thus, they most likely represent partial melts of an Ab-Or-mafic mineral(s) mixture.

Significance: The ~4.6 Ga age of the Adzhi-Bogdo zircon indicates that: 1) moderately volatile elements were retained in melts through some high temperature events in the early solar system; and, 2) the clast (breccia) has not been heated above ~970 °C since crystallizing based on diffusion calculations for a 30 μm zircon (min. T using a low 10°C/Ma cooling rate [6]). We speculate that the melts in the LL meteorites and high pressure mantle crystals formed by partial melting near the Ab-Or thermal divide (>~1060°C) at slightly lower or similar temperature to core formation (Fe melts at ~1400°C dependent on oxidation; [7]). The results support the idea that parent body differentiation was a very early process [8] and suggest that any first-generation planetesimals re-accreted at temperatures below ~970 °C.

References: [1] Jäckel, A. & Bischoff, A., 1997. Abstr. #5072. 60th Meteoritical Society Meeting. [2] Bischoff, A. et al., 1993. *Meteoritics* 28:570-578. [3] Ivanov, A. V. et al., 2001. Abstr. #1386. 32nd Lunar Planetary Science Conference. [4] Wlotzka, F. et al., 1983. *Geochimica et Cosmochimica Acta* 47:743-757. [5] Schiano, P. & Bourdon, B., 1999. *Earth & Planetary Science Letters*, 169:173-188. [6] Cherniak, D. J. & Watson, E. B., 2003. Diffusion in Zircon, *Reviews in Mineralogy & Geochemistry*, 53: 113-143. [7] Darken L. S. & Gurry R. W. (1945) *Journal American Chemical Society* 67, 1398-1412. [8] Kleine, T. et al., 2005. Abstr. #1431, 36th Lunar Planetary Science Conference.

INTERNAL HEATING OF THE UREILITE PARENT BODY

BY SHORT-LIVED NUCLIDES. N. T. Kita¹, Y. Ikeda², G. Shimoda³, S. Togashi³, Y. Morishita³ and M. K. Weisberg⁴,
¹University of Wisconsin-Madison. ²Ibaraki University.
³Geological Survey of Japan. ⁴Kingsborough College (City University New York).

Introduction: Polymict ureilites contain a variety of feldspathic clasts containing plagioclase, which may be related to the “missing basalt” components of the ureilite parent body (UPB) [1-2]. The ²⁶Al ages of several feldspathic clasts in DaG-319 showed ages of ~5.2 million years (My) after CAI formation and are indistinguishable from each other [3]. These ages are consistent with the ⁵³Mn ages of similar clasts in DaG-319 and DaG-165 [4] and the 4,563±6 My Pb-Pb age of the MET78008 monomict ureilite [5]. All of these results indicate early igneous activity on the ureilite parent body. In this study, internal heating of the UPB by the short-lived nuclides ²⁶Al and ⁶⁰Fe are examined and compared to the ²⁶Al ages of feldspathic clasts [3] and the smelting model by Singletary and Grove [6].

Thermal model of UPB: A simple thermal model of the UPB is considered. The initial abundance of the ²⁶Al and ⁶⁰Fe are assumed to be ²⁶Al/²⁷Al=5×10⁻⁵ [7] and ⁶⁰Fe/⁵⁶Fe=(5-10)×10⁻⁷ [8], respectively. The final internal temperatures of ferroan and Mg-rich monomict ureilite sources should reach 1220°C and 1300°C, respectively [6]. We examined two models for interpretations of the ²⁶Al ages of the feldspathic clasts (5.2 My after CAIs). Model-1: The parental magma for the feldspathic clasts was generated at 5.2 My with a temperature of ~1150°C [2]. Model-2: The UPB was disrupted by an impact at 5.2 My and the feldspathic clasts solidified during the subsequent rapid cooling of the UPB. We also considered various cases where silicate partial melts are removed and redistributed within UPB.

Results and Discussions: Model-1: The internal temperature of the UPB could reach 1150°C at 5.2 My if the parent body formed and started to retain heat at 2.2-2.5 My after CAI formation. However, it is difficult to explain the final temperature of the Mg-rich monomict ureilite source region unless a large portion of melt component with ²⁶Al was added. It might take at least 7 My after CAIs to reach the final temperatures. Model-2: The parental magma of the feldspathic clasts could be generated at ~4.5 My and the final temperature of the ferroan monomict ureilite source could reach 1220°C at 5.2 My if the UPB started 2.1-2.4 My after CAIs. The Mg-rich monomict ureilite source needs an additional melt component with ²⁶Al to reach the final temperature as in the case of Model-1. It is not clear if the petrography and chemistry of the feldspathic clasts are consistent with rapid crystallization by impact disruption of the UPB. In both models, timing of UPB formation (~2 My) might have overlapped with the late stages of chondrule formation [e.g., 9].

References: [1] Ikeda Y. et al. 2000. *Antarctic Meteorite Research* 13:177-221. [2] Kita N. T. et al. 2004. *Geochimica et Cosmochimica Acta* 68:4213-4235. [3] Kita N. T. et al. 2003. Abstract #1557. 34th Lunar & Planetary Science Conference. [4] Goodrich C. A. et al. 2002. *Meteoritics & Planetary Science* 37:A54. [5] Torigoye-Kita N. et al. 1995. *Geochimica et Cosmochimica Acta* 59:381-390. [6] Singletary S. J. and Grove T. L. 2003. *Meteoritics & Planetary Science* 38:95-108. [7] MacPherson G. J. et al. 1995. *Meteoritics* 30:365-386. [8] Tachibana S. 2005. Abstract #1529. 36th Lunar & Planetary Science Conference. [9] Kita et al. 2005. Abstract #1750. 36th Lunar & Planetary Science Conference.

MAGNETIC PALEOFIELD ESTIMATES FOR CHONDRULES EXTRACTED FROM BJURBOLE (L4) METEORITE. G. Kletetschka^{1,2,3}, P. T. Wasilewski² V. Zila⁴,
¹Catholic University, Washington DC, USA, gunther.kletetschka@gsfc.nasa.gov, ²NASA-GSFC, Greenbelt, MD, 20771, USA, ³Institute of Geology ASCR, Prague, Czech Republic ⁴ Charles University, Prague, Czech Republic.

Introduction: Paleomagnetic intensity estimates from meteorites contain constraints for solar system evolution. Ordinary chondrites (H, L, and LL types), are the materials most likely matched with the S-type asteroids and their magnetism is due to Fe-Ni compounds, primarily α -kamacite (<7% Ni), γ -taenite (>7% Ni), and γ'' -tetrataenite (43-52% Ni).

Acquisition of magnetism during the residence inside the geomagnetic field: Previous magnetic study of Bjurbole (L4) chondrules [1] described very stable remanence directions even after AF demagnetization with 0.24 T. We examined [2] the magnitude of terrestrial contamination associated with the entry of meteorites from space into the terrestrial environment. Most of our experimental magnetic work was done on individual chondrules from Bjurbole (L4) ordinary chondrite. It is classified as an L4 and is very friable. Even though separated chondrules are small (1-50 mg) they still contain significant magnetization measurable with our superconducting rock magnetometer (SRM) which is part of Goddard magnetic facility. Remanent magnetization was removed in very detailed field steps by alternating field demagnetization.

Results: Warming up from space temperatures and an exposure to geomagnetic field environment during the meteorite entry influenced magnetism of some chondrules. Other chondrules were relatively unaffected. Low temperature treatment had negligible effect on their magnetic remanence. These stable chondrules were selected for paleofield estimates.

We detected thermal/chemical type of remanence and distinguished it from isothermal remanent magnetization [3]. According to this method two chondrules in our analysis contain TRM/CRM as one stable magnetic component. Another chondrule indicates continuous decay of paleofield value indicating magnetic exposure to later fields of ~100 mT.

Paleofield estimate:: The paleofield method based on the efficiency ratio [4] reveals paleofields between 12 μ T and 45 μ T (REM ~ 0.0015-0.0048) for three chondrules.

Conclusions: Magnetic record of the Bjurbole chondrite and by analogy perhaps all meteorites is complicated by the fact that it contains magnetic material capable of acquiring a wide range of magnetic remanence records by warming from space temperature and magnetic conditions to 300K inside the terrestrial environment. We were able to select a significant fraction of chondrules that contains stable remanent directions that is unlikely to be contaminated by exposure to geomagnetic field and terrestrial temperatures. We show that this record is due to thermal/chemical magnetization acquisition and that the acquisition field was close to terrestrial values (15000-45000 nT).

References: [1] Wasilewski, P. et al. (2000) *Meteoritics and Planetary Science*, 35, 537-544. [2] Kletetschka et al, 2001, 32nd LPSC #1958. [3] Kletetschka et al, 2005, IAGA abstract (Toulouse) [4] Kletetschka G. et al. 2004. *EPSL* 226: 521-528.

TEKTITES: WHY ARE THEY ON THE EARTH, BUT NOT ON THE MOON?

Christian Koeberl, Department of Geological Sciences, University of Vienna, Althanstrasse 14, A-1090 Vienna, Austria (christian.koeberl@univie.ac.at).

Tektites are a group of natural glasses that have puzzled mankind for many centuries. After centuries of collecting, and decades of study, we are now closer to an understanding of their origin. First, though, what are tektites? They are chemically homogeneous, often spherically symmetric objects that are in general several centimeters in size, and occur in four known strewn fields on the surface of the Earth. Strewn fields can be defined as geographically extended areas (in the case of tektites larger than just a few square kilometers) over which tektite material can be found. Four such strewn fields (all of Cenozoic age) are known (North American, Central European, Ivory Coast, and Australasian). Traditionally there have been four explanations for the possible origin of tektites – that they are ejecta of impacts or volcanic eruptions on the Earth or the Moon. Until the 1960s, the lunar volcanic hypothesis was predominant. Any discussion of the origin of the tektites needs to explain the similarity of tektites in respect to age and certain aspects of isotopic and chemical composition within one strewn field as well as the existence of tektite material with different compositions present in each strewn field. In general, the major and trace element composition of tektites is almost identical to the composition of the terrestrial upper crust. This fundamental observation was made mainly by S.R. Taylor and co-workers, who, during the 1960s and 1970s, have performed detailed geochemical studies of many tektite types. Mainly due to these and later chemical and isotopic studies, it is now commonly accepted that tektites are the product of melting and quenching of terrestrial rocks during hypervelocity impact on the Earth. The determination of the exact source rocks of tektites is complicated because a variety of target rocks was apparently sampled by each impact event. However, for three of the four strewn fields, source craters have been identified already based on chemical, isotopic, and chronological arguments. Numerical simulation calculations even provide plausible mechanisms that explain how tektites form during an impact event. If tektites are just early-phase distal impact ejecta, the question arises why they have not been found on the Moon. There are probably several answers to that question. First, finding tektites on the Earth by chance on a few selected places are near zero – just as they might be on the Moon, finding tektites at the few Apollo and Luna landing places. Tektites are rare on Earth, too. Second, tektites on the Moon would be different anyway, because surficial melts on the Moon would be made from the lunar surface – mostly regolith – and would, thus, be rich in meteoritic material (tektites on Earth have a very small meteoritic component). Also, tektites on the Moon would have a totally different composition than on the Earth, with no rocks similar to the silica-rich terrestrial upper crustal rocks present. There are some gram-sized melt bombs in the Apollo 16 collection, possibly from the (nearby) South Ray crater, and some small ropy glasses in the Apollo 12 collection, which might be ejecta in a ray from Copernicus, but all this needs to be quantified and confirmed if such glasses could represent tektite analogs. One conclusion remains: tektites are a „local“ product and did not travel through interplanetary space.

Acknowledgments: The author wants to thank S.R. Taylor for decades of important scientific contributions and friendship.

DISCRIMINATING GLASSES AND PHYLLOSILICATES IN THERMAL INFRARED DATA.

W. C. Koeppe and V. E. Hamilton. Hawaii Institute for Geophysics and Planetology, 1680 East-West Rd, POST 504, Honolulu, HI 96822. E-mail: koeppe@higp.hawaii.edu.

Introduction and Approach: Thermal infrared spectra of glasses and phyllosilicates have similar shapes leading to a proposed ambiguity in deconvolution results [1]. We quantify the spectral separability and uncertainty of these two classes using discriminant analysis [2] and linear deconvolution [3, 4]. We apply the deconvolution technique to single spectra, and two- and four-component numerical mixtures using multiple end-member sets that include or exclude mixture components. Missing end-members result in uncertainties in the modeled abundances of glasses and phyllosilicates.

Conclusions: Even though the spectra of glasses and phyllosilicates appear similar, discriminant analysis shows they are statistically separable. If the deconvolution algorithm is given all possible end-members, and minerals in a mixture are similar to those in the end-member set, results closely approximating the actual abundances are achieved. If differences exist between glasses and phyllosilicates in the mixture and those in the end-member set, uncertainties arise. Mixtures containing saponite, nontronite, and halloysite showed the highest errors in reported abundances of glasses and phyllosilicates where the phyllosilicate in the mixture was not present in the end-member set. Silica-K₂O glass is more susceptible to being modeled by phyllosilicate minerals than pure silica glass. When silica-K₂O glass is in the mixture but excluded from the end-member set used to deconvolve the mixture, phyllosilicates erroneously model the silica-K₂O spectral shape by up to 60%, sometimes with only a minimal increase in RMS error. We show that glasses and phyllosilicates in simple four-component mixtures act as a two-component system and are anti-correlated. As a result, their absolute deconvolved abundances are subject to uncertainties based on the total amount of glass and phyllosilicate in the mixture. Applying these uncertainties to the results of [4], we find that the modeled glass abundance in the surface type 2 spectrum is well above the detection limit of TES if the silica-K₂O glass is representative of glasses on Mars. Phyllosilicate abundances for surface type 2 remain at or below the detection limit even with the maximum uncertainties in deconvolved abundances applied. Our analyses indicate that amorphous silica weathering products with band minima similar to the pure silica glass [5, 6] are the glasses least likely to be confused with phyllosilicates. Good spectral fits to Martian spectra indicate that pure silica glass, if present on the surface of Mars, is a small (less than ~5-10%) component of the global spectral shapes. Both primary volcanic or secondary weathering phases with spectral characteristics like the silica-K₂O glass provide viable explanations for the origin of this component on Mars.

References: [1] Wyatt M. B. and H. Y. McSween, Jr. 2002. *Nature*, 417:14711-14732. [2] Rencher, A. C., 1995. Wiley Interscience, New York, 627pp. [3] Ramsey, M. S. and P. R. Christensen. 1998. *Journal of Geophysical Research*. 103 (B1), 577-596. [4] Bandfield et al. 2000. *Science*. 287, 1626-1630. [5] Kraft et al. 2003. *Geophysical Research Letters*. 30: 24, 10.1029/2003GL018848. [6] Michalski et al. 2003. *Geophysical Research Letters*. 30:19, 10.1029/2003GL018354.

THE GLOBAL DISTRIBUTION OF OLIVINE ON MARS: FORSTERITE TO FAYALITE. W. C. Koepfen and V. E. Hamilton. Hawaii Institute for Geophysics and Planetology, 1680 East-West Rd, POST 504, Honolulu, HI 96822. E-mail: koepfen@higp.hawaii.edu.

Introduction: Olivine has been identified in Mars Global Surveyor Thermal Emission Spectrometer (MGS TES) data in concentrations up to ~30% [1, 2]. [1] identified multiple compositions in Nili Fossae and Syrtis major using spectral feature mapping (or band indices) [3], whereas [2] reported on the global distribution of olivine that matched the spectral signatures of the Chassigny and ALH A77005 (Fo₆₈) Martian meteorites. [3] reported on global olivine band index maps, but these data have not been published and are not publicly available. Global maps of olivine also were made using the forsterite and fayalite of the TES ASU spectral library [4]; however, intermediate compositions of olivine cannot be made by simple addition of the compositional end-members.

Approach: In addition to the olivines in the ASU spectral library [5], we prepared and analyzed emission spectra of a suite of particulate olivine samples from the Kiglapait Intrusion in Labrador described (and provided) by [6] to map the global distribution of all separable compositions of olivine from TES data. The Kiglapait samples add the following Fo numbers to our collection: 68, 60, 53, 39, 35, 25, 18, 10. Our approach is twofold. First, we have created qualitative global maps of each solid solution composition based on band indices. Indices for close compositional ranges use complex ratios or multiplicative factors of spectral features in spectral regions where atmospheric contributions to surface spectra are minimized. We selected these features to discriminate multiple compositions and exclude false identifications of other minerals, as tested against the ASU spectral library [5]. We calculated each index for all TES data meeting minimum quality constraints and then made global maps that we compared to previous identifications [e.g., 1, 2]. Maps were then verified via inspection of individual spectra. The second step in our approach will consist of linearly deconvolving the TES data [e.g., 2, 4] using these olivines and a mineral library to create global maps of olivine distribution and concentration.

Results: The index for Fo₉₁ is the least ambiguous index and shows possible concentrations in Argyre and Hellas basins, Nili Fossae, and Arcadia Planitia. Fo₆₀₋₆₈ maps agree with previous identifications by [2] in Nili Fossae, southwestern Isidis rim, Ganges and Eos Chasmata craters in Aurorae Planum, and isolated regions in Noachis Terra. Identifications of Fo₅₃ are restricted to isolated pixels and possible detections in the Valles Marineris, near Elysium, and Acidalia Planitia. Olivine of composition Fo₂₅₋₃₉ and Fo₁₈ for the most part follow the trend of TES surface type 1 (basalt). Fayalite index maps resemble maps of hematite, a mineral which may be obfuscating the detection of iron-rich olivine based on these indices.

References: [1] Hoefen, T. M. 2003. *Science*, 302, pp. 627-630. [2] Hamilton et al. 2003. *Meteoritics & Planetary Science*, 38:6, pp. 871-885. [3] Clark, R. N. and T. M. Hoefen. 2000. *Bulletin of the American Astronomical Society*. 32:1118. [4] Bandfield, J. L. 2002. *Journal of Geophysical Research*. 107:E6, 5042, 10.1029/2001JE001510. [5] Christensen et al. 2000. *Journal of Geophysical Research*. 105:E4, pp. 9735-9739. [6] Morse, S. A., *Journal of Petrology*, 37:5, pp. 1037-1061.

CHONDRULE MAGNETIC CONGLOMERATE TEST OF AVANHANDAVA H4 CHONDRITE. T. Kohout^{1, 2, 3} and Lauri J. Pesonen². ¹Division of Geophysics, Faculty of Science, University of Helsinki, Finland. E-mail: tomas.kohout@helsinki.fi. ²Department of Applied Geophysics, Faculty of Science, Charles University in Prague, Prague, Czech Republic. ³Institute of Geology, Academy of Sciences of the Czech Republic, Prague, Czech Republic.

Introduction: The Avanhandava (H4) fall occurred in 1952 in Brazil. A total of 9.33 kg had been preserved after the meteorite broke up during the impact [1]. The bulk petrophysical parameters (density 3.39 g/cm³ and magnetic susceptibility 0.73 SI) reflect H4 range [5]. The meteorite contains large (0.1 – 2.0 mm) chondrules that have clearly delineated boundaries with matrix. This characteristic allows us to pick up oriented individual chondrules and study their magnetic properties.

Magnetic properties of chondrules and matrix: The chondrules carry a weak NRM (Natural Remanent Magnetization) in order of 10⁻² – 10⁻¹ mA/m²/kg, low coercivities (< 10 mT) and a low J_{sr} to J_s (saturation remanent magnetization to saturation magnetization) ratio (~10⁻²). The matrix carries two orders of magnitude higher NRM values (10⁰ – 10¹ mA/m²/kg), slightly higher coercivities (~30 mT) and a higher J_{sr} to J_s ratio (~10⁻¹). From the temperature dependence of magnetic susceptibility data Fe-Ni alloy was identified in chondrules and matrix. The matrix shows remarkable traces of terrestrial weathering (ochre tint) and the contribution of magnetite (probable weathering product) was observed in susceptibility data. The NRM of both the chondrules and the matrix is mostly stable up to 10 mT alternating field.

Chondrule magnetic conglomerate test: The chondrule magnetic conglomerate study was done by removing oriented chondrules from the meteorite matrix and comparing the direction of their NRM with respect to each other and to the matrix. The direction of the NRM of the chondrules seems to be randomly oriented within the meteorite. In contrast the neighboring matrix fragments show consistent directions of the NRM vectors.

Paleofield estimate: The paleofield method based on the REM ratio (NRM/J_{sr}) [2] reveals approximate paleofields between 5 μT and 20 μT (REM ~ 0.002) for chondrules. The REM value (~ 0.02) of the matrix is in the range observed on terrestrial rocks.

Conclusions: The chondrules of the Avanhandava meteorite show a low and randomly oriented NRM and the paleofield determined is almost one order of magnitude lower than geomagnetic field. That suggests that chondrules are not magnetically contaminated by geomagnetic or artificial fields and they acquired their NRM prior their aggregation to Avanhandava parent body. The matrix shows remarkable traces of terrestrial weathering and is strongly magnetized in one direction what together with the REM value characteristic for terrestrial rocks can be a result of remagnetization during terrestrial weathering. The terrestrial weathering of ordinary chondrites is observed even on falls stored in museums and can significantly influence meteorite magnetic records [3, 4].

References: [1] Paar W. et al. 1976. *Revista Brasileira de Geociencias* 6: 201–210. [2] Kletetschka G. et al. 2003. *Meteoritics & Planetary Science* 38: 399-405. [3] Kohout T. et al. 2004. *Physics and Chemistry of the Earth* 29: 885-897. [4] Lee M. R. and Bland P. A. 2004. *Geochimica et Cosmochimica Acta* 68: 893-916. [5] Terho M. et al. 1993. *Studia Geophysica et Geodaetica* 37: 65-82.

CRYSTALLIZATION OF LUNAR MARE METEORITE

LAP 02205. E. Koizumi, J. Chokai, T. Mikouchi, J. Makishima and M. Miyamoto. Dept. of Earth and Planet. Sci., University of Tokyo, Hongo, Tokyo 113-0033, Japan. E-mail: koi@eps.s.u-tokyo.ac.jp

Introduction: LAP 02205 (LAP) is the newest member of crystalline lunar mare meteorites mainly consisting of pyroxene, plagioclase and olivine. Pyroxenes are extensively zoned from Mg-rich pigeonite cores ($\text{En}_{55}\text{Fs}_{30}\text{Wo}_{15}$) to nearly Mg-free rims via augite mantles ($\text{En}_{40}\text{Fs}_{25}\text{Wo}_{35}$). Rare olivine grains are zoned from Fo_{67} cores to Fo_{48} rims. Since LAP does not show a typical cumulate texture, its bulk composition might retain its parent melt composition. In this study, we investigated the crystallization history of LAP by using MELTS calculation and performing crystallization experiments.

MELTS calculation: We calculated equilibrium mineral assemblages by the MELTS program with the LAP bulk composition [1]. The calculation results show that the liquidus phase is olivine (Fo_{55}) at 1137 °C. Then, olivine immediately disappears and pigeonite ($\text{En}_{53}\text{Fs}_{36}\text{Wo}_{11}$) starts crystallizing at 1134 °C. Olivine composition is more Fe-rich than that of the olivine core in LAP, although pigeonite compositions are similar between calculated and pigeonite core in LAP. This result shows that the core composition of olivine in LAP is too magnesian to be crystallized from the LAP bulk composition, and Mg-rich olivine cores are xenocrysts.

Crystallization experiments: We performed crystallization experiments with the LAP bulk composition in 1 atm vertical furnaces [2]. Homogenized starting glass was cooled from 1155 °C to 1000 °C at various cooling rates (1, 2.5, 5, 10, and 20 °C/hr) under $\log f\text{O}_2 = \text{IW}-1$. All run products contained olivine, pyroxene, plagioclase and ilmenite. The textures and pyroxene compositions of run products from 1 to 10 °C/hr cooling runs were generally similar to those of LAP. However, the run product from 20 °C/hr cooling run showed a different texture (skeletal olivine, acicular plagioclase) and pyroxene composition was more Ca-rich. The largest difference among each cooling run is in olivine petrology. In slower cooling experiments, the amount and grain size of olivine were smaller and their compositional ranges were narrower. The core compositions of these olivines are Fo_{58} . This composition is more Fe-rich than that of LAP, indicating the xenocryst origin of Mg-rich olivine in LAP. We also performed 1 °C/hr cooling experiment quenched at 1130 °C. There were many large olivine grains (Fo_{57-49}) in the run product in contrast to the 1 °C/hr cooling run down to 1000 °C. These results show that olivine melted with the pyroxene crystallization as MELTS calculation predicts.

Discussion and conclusion: Although the Mg-rich cores of olivine could be xenocrysts, the amount of olivine is small and has little influence on the LAP bulk composition. Probably, the LAP bulk composition is similar to its parent melt composition. The crystallization experiment shows that LAP should have been cooled fast enough to preserve olivine from complete melting. Thus, the pyroxene and olivine mineralogy of experimental charges suggest 1-5 °C/hr cooling rate during the crystallization of the LAP magma.

References: [1] Ghiorso M. S. and Sack R. O. 1995. *Contribution to Mineralogy and Petrology* 119:197-212. [2] McKay G. et al. 1994. *Geochimica et Cosmochimica Acta* 58:2911-2919.

GEOCHEMICAL EVIDENCE FOR THE NOVAYA YERGA METEORITE FALL, 1660s.

A. V. Korochantsev, C. A. Lorenz, M. A. Ivanova, and M. A. Nazarov. Vernadsky Institute, Kosygin St., 19, Moscow 119991. E-mail: meteorites@geokhi.ru

Introduction: A letter dating from the 1660s describes a phenomenon similar to a meteorite fall near Novaya Yerga, Russia [1]. However, no meteorite material has been found in the area. We investigated Ni and Ir distribution in soil collected near Novaya Yerga (59° 23' N; 37° 51' E). Results suggest a meteorite fall took place.

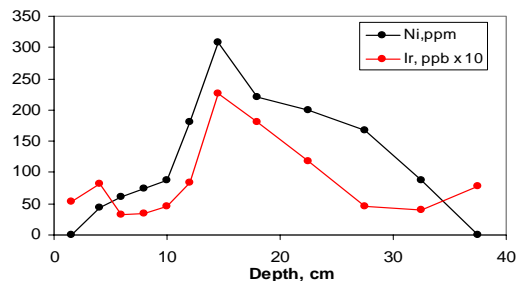
Results: Meteorites lose 30-60% of their mass to ablation [2], and the mass of ablated dust inside a spreading area is comparable to the mass of fallen fragments [3]. The strewn field of ablation dust, enriched in siderophile elements, is much bigger than the fragment field. Thus, siderophile element enrichments in recent sediments could be indicative of historical meteorite falls.

We sampled a column (40 cm) of floodplain deposits of the Chermasola River near Novaya Yerga. The sampling strategy was based on the following reasons: (1) the Chermasola deposits an annual spring flood layer and therefore the floodplain stratigraphy is a record of historical time; (2) the apparent meteorite fall was in December, 1662, so when the snow melted in the spring of 1663, the meltwater should have redeposited any extraterrestrial material from neighboring elevations down to the Chermasola floodplains; (3) the floodplains around Novaya Yerga were generally not used for farming, so the yearly layers should have remained largely unmixed.

We separated magnetic fractions from the samples because ablation dust should be concentrated in the magnetic fractions. These were then analyzed by INAA to measure Ni and Ir content.

Discussion: The average concentrations of Ni (0.73 ppm) and Ir (0.03 ppb) in the soil were calculated from the contents of magnetic fractions in all layers. These concentrations don't exceed average Ni and Ir concentrations of upper earth crust (15 ppm and 0.02 ppb). However, their Ir/Ni ratio is similar to CI chondrites (4.4×10^{-5}). The magnetic fraction from the 13-16 cm layer is enriched in Ni (308 ppm) and Ir (22.8 ppb) compared to those from other layers (Fig.). Therefore this layer could be a buried surface of ablation dust deposition. The integrated surface concentration of all layers (1.4 ng/cm^2) is comparable with that of K/T boundary ($>3 \text{ ng/cm}^2$ [4]). Thus we conclude that the sampled soil appears to contain chondritic material, a possible record of a historical Novaya Yerga meteorite fall.

References: [1] Svyatsky D. O. (1936?). *Mirovedenie*, XVIII, 5 (in Russian). [2] Lovering J. F. et al. (1960) *Geochim. et Cosmochim. Acta* 19, 156-158. [3] Lorenz C.A. et al. 1998. *Meteoritics and Planetary Sciences* 33, A95. [4] Donaldson S.J. et al. (2001) *Meteoritics and Planetary Sciences* 36, A50.



THE MYTH OF THE MAGNESIAN SUITE OF LUNAR "HIGHLANDS" ROCKS

R. L. Korotev. Department of Earth and Planetary Sciences, Washington University, Saint Louis, Missouri. E-mail: korotev@wustl.edu.

Introduction: On the basis of Apollo samples, igneous and plutonic rocks of the lunar crust have long been divided into two main petrogenetic groups, the ferroan-anorthositic ("ferroan anorthosite") suite and the magnesian ("Mg-rich," "magnesium") suite [1,2]. The latter consists mainly of mafic plutonic rocks like norite, troctolite, dunite, and gabbro but also alkaline anorthosite and KREEP basalt [2]. Although early works conservatively designated such rocks only as "nonmare" [1], the magnesian suite is usually identified with the feldspathic highlands [e.g., 2–5]. New data suggest a different heritage.

Orbital Geochemistry and Mineralogy: Various studies have shown that the Apollo magnesian-suite rocks differentiated from KREEP (Th-rich) magmas. Lunar Prospector demonstrated that KREEP is almost entirely restricted to the PKT (Procellarum KREEP Terrane), a unique geochemical province [6]. There is no evidence in the LP data that KREEP is globally distributed beneath the FHT (Feldspathic Highlands Terrane) [7]. There is no evidence in the Clementine data for intrusions of truly mafic plutons (norite, troctolite, gabbro) into the feldspathic crust [8].

Lunar Meteorites: Feldspathic lunar meteorites, all of which are polymict breccias, derive from numerous places in the FHT. Mafic magnesian-suite rocks such as those of the Apollo missions are absent as clasts in the meteorites; they are only common at Apollo sites in or near the PKT [9].

Conclusions: Magnesian-suite rocks are not rocks of the lunar highlands, and it can (and has) only lead to obfuscation to regard them as such. They are products of the Procellarum KREEP Terrane, a topographically low region that is distinct from the feldspathic highlands [6,10,11]. The misconception arises from preconception, historical accident, coincidence, and non-ideal order of discovery [12]: (1) The Moon has long been viewed as simply bimodal in geology, mare or highlands; (2) The last basin-forming bolide to strike the lunar nearside happened to impact the PKT, redistributing Th-rich material about the surface [13]; (3) All six Apollo landings occurred in or near the PKT; (4) The Apollo samples (unlike as for Mars) were acquired, studied, and interpreted long before global constraints imposed by orbital missions and lunar meteorites were obtained.

Magnesian (high-Mg/Fe) feldspathic lithologies exist in the highlands, but there is no evidence that such lithologies are related to the magnesian suite of the PKT and nearly all such samples are brecciated [9].

References: [1] Warren PH & Wasson JT (1977) *PLSC8*, 2215–2235. [2] Papike JJ et al. (1998) *Reviews in Mineralogy* **36**, 5–1–5–234. [3] Taylor SR et al (1993) *Meteoritics* **28**, 448. [4] Shearer CK & Papike JJ (1999) *Am Min* **84**, 1469–1494. [5] Cahill JT et al. (2004) *M&PS* **39**, 503–530. [6] Warren PH (2004) Vol. 1, 559–599. *Treatise on Geochemistry*. [7] Jolliff BL et al. (2000) *J Geophys. Res.* **105**, 4197–4416. [8] Lawrence DJ et al. (2000) *JGR* **105**, 20,307–20,331. [9] Tompkins S & Pieters CM (1999) *M&PS* **34**, 25–41. [10] Korotev RL et al. (2003) *GCA* **67**, 4895–4923. [11] Korotev RL (2000) *JGR* **105**, 4317–4345. [12] Korotev RL & Gillis JJ (2001) *JGR* **106**, 12,339–12,353. [13] Korotev RL (submitted) *Chemie der Erde*. [14] Haskin LA (1998) *JGR* **103**, 1679–1689.

ION IMPLANTATION INTO NANODIAMONDS AND THE MECHANISM OF HIGH TEMPERATURE RELEASE OF NOBLE GASES FROM METEORITIC DIAMONDS. A. P. Koscheev¹, M. D. Gromov¹, P. V. Gorokhov¹, U. Ott², G. R. Huss³, and T. L. Daulton⁴. ¹Karpov Institute of Physical Chemistry, Vorontsovo Pole 10, 105064, Moscow, Russia. E-mail: koscheev@cc.nifhi.ac.ru. ²Max-Planck-Institut für Chemie, Becherweg 27, D-55128 Mainz, Germany. ³HIGP, Univ. of Hawai'i at Manoa, Honolulu, HI, 96822, USA. ⁴Naval Research Laboratory, Stennis Space Center, MS 39529-5004, USA.

Introduction: Presolar meteoritic diamond grains are the carriers of different components of noble gases [1] trapped most probably by ion implantation [2]. The isotopically unusual HL component releases at high temperatures (HT) above 1200°C during pyrolysis [1]. The mechanism of this HT release from nanodiamonds is not well understood. Using noble-gas ion implantation into synthetic diamonds we have studied the details of HT release compared to the case of meteoritic diamonds.

Results and Discussion: Stepped pyrolysis measurements (100°C steps) of ion implanted synthetic diamonds indicated that the "median temperature" (T_m) of the HT peak increased from Ar to Xe. The differences between T_m were 16°C and 33°C for Kr-Xe and Ar-Kr, respectively. Careful analysis of noble gas data for nine types of meteoritic nanodiamonds measured by similar protocol [1] showed the same trend in most cases for Ar-Kr (-10 to 18°C) and in all cases for Kr-Xe (10 to 34°C).

These differences in T_m were confirmed for ion-irradiated synthetic nanodiamonds by a new measuring procedure with high temperature resolution (17°C). The HT release of trapped gases appears unique for nanostructured diamonds (as it was not observed in micron-sized diamonds) and could relate to the transformation of nanodiamonds into an onion-like graphitic structure during high temperature annealing [3]. TEM studies of the nanodiamonds, as used in our implantation experiments, showed that annealing at 700 °C in vacuum was sufficient to transform some nanodiamonds to onion-like graphites, perhaps initiated by amorphization. Further, at 1500 °C most nanodiamonds were transformed. The observed differences of T_m for different gases might be explained by different ion penetration depths increasing in the sequence Ar-Kr-Xe, according to the TRIM calculations for bulk materials. We observed that the HT peak shifts to higher temperatures (from 1467 to 1553°C for Ar) with ion energy in the range 250-3000eV, possibly reflecting the increase in ion penetration depth. Ion implantation into nanodiamonds pre-annealed at 1200 and 1400°C showed a substantial decrease of HT peak with annealing temperature, consistent with a decreasing diamond/graphite ratio.

Large differences (up to 120°C) in T_m of the HL-Xe peak in diamonds from different meteorites [1] could be explained by a range of ion-implantation energies coupled with natural sorting of diamonds. The T_m for gas release correlates with the metamorphic grade of the host meteorite [4]. Preferential destruction of smaller grains or poorly crystalline grains, those less able to capture high-energy ions, could shift the T_m of the surviving diamonds. A range of implantation energies implies that for meteoritic diamonds with low or even negative shift of T_m for Ar-Kr [1], HL-Ar was implanted at higher energy than Kr and Xe.

References: [1] Huss G. R. and Lewis R. S. 1994. *Meteoritics* 29:791-810. [2] Koscheev A. P. et al. 2001. *Nature* 412:615-617. [3] Kuznetsov V. L. et al. 1994. *Chem. Phys. Lett.* 222:343-348. [4] Huss G. R. and Lewis R. S. 1994, *Meteoritics* 29:811-829. **Acknowledgments:** Supported in part by RFBR-DFG (grant 02-05-04001) and by NASA (contract W-10246 through OSS).

COARSE-GRAINED ANORTHITE-RICH (TYPE C) CAIS IN CARBONACEOUS CHONDRITES: EVIDENCE FOR A COMPLEX FORMATION HISTORY. A. N. Krot¹, H. Yurimoto², M. I. Petaev³, I. D. Hutcheon⁴, D. A. Wark⁵, G. Libourel⁶, L. Tissandier⁶, and J. M. Paque⁷. ¹University of Hawai'i at Manoa, USA. ²Hokkaido University, Japan. ³Harvard University, USA. ⁴Lawrence Livermore National Laboratory, USA. ⁵Monash University, Australia. ⁶CRPG/CNRS, France. ⁷California Institute of Technology, USA.

Introduction: Coarse-grained, igneous, anorthite-rich (Type C) CAIs have been initially recognized in the CVs [1,2], and subsequently described in the CRs [3], COs [4], and Ningqiang [5]. Because relict spinel-plagioclase-pyroxene CAIs are commonly observed in the Al-rich chondrules in CVs [6] & CRs [7], and bulk compositions of Type C CAIs are close to those of some of the Al-rich chondrules [e.g., 6-8], Type C CAIs can potentially provide a clue for a genetic relationship between refractory inclusions and chondrules. In order to understand the origin of Type C CAIs in CCs, we initiated detailed study of their mineralogy, trace elements, O- and Al-Mg isotopic compositions.

Results: (i) Three Type C CAIs from Allende (ABC, TS26, 93) and all three Type C CAIs found in CRs [3] experienced late-stage remelting in an ¹⁶O-poor nebular gas, with or without addition of chondrule-like ferromagnesian materials, probably in the chondrule-forming region [9,10]. (ii) Type C CAIs 100, 160, and 6-1-72 from Allende consist of very fine-grained (<5 μm) anorthite groundmass surrounding coarse-grained Na- and Åk-rich melilite and Al-Ti-diopside with numerous μm-sized inclusions of anorthite, and relict(?) regions composed of coarse-grained, massive Al-Ti-diopside and gehlenitic melilite, and spinel palisades. We infer that these CAIs formed by remelting of Type B CAIs which experienced either extensive replacement of melilite by anorthite and nepheline(?) prior to melting or condensation of gaseous SiO and Na into Type B CAI melts. (iii) Type C CAI CG5 consists of coarse anorthite, gehlenitic melilite, and Al-Ti-diopside, all poikilitically enclosing numerous spinel grains, and may have formed by melting of fine-grained spinel-rich CAI which experienced extensive replacement of melilite by anorthite.

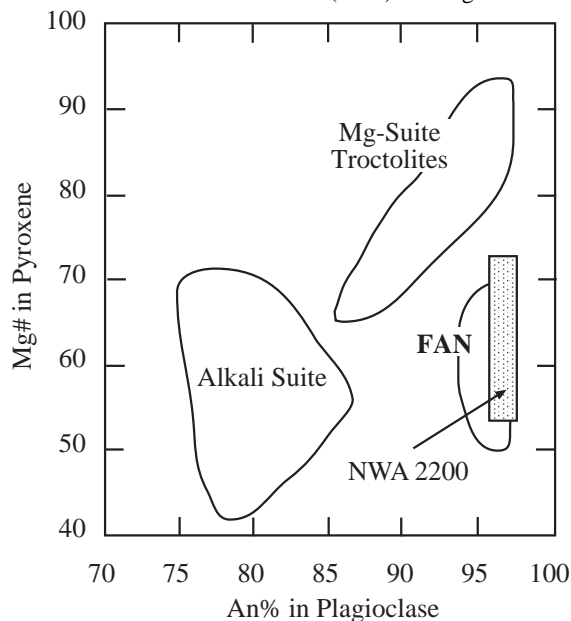
While Type C CAIs in CRs are mineralogically pristine, the Allende Type C CAIs experienced multistage alteration history, including replacement of melilite and anorthite by grossular, monticellite, forsterite, and wollastonite, followed by an Fe-alkali metasomatic alteration resulting in formation of sodalite, nepheline, ferrous olivine, hedenbergite, and andradite. Melilite-anorthite assemblages in ABC, TS26, and 93 are replaced by grossular, monticellite, and wollastonite, suggesting an isochemical reaction: $4\text{Ca}_2\text{MgSi}_2\text{O}_7 + \text{Ca}_2\text{Al}_2\text{SiO}_7 + \text{CaAl}_2\text{Si}_2\text{O}_8 = 2\text{Ca}_3\text{Al}_2\text{Si}_3\text{O}_{12} + 4\text{CaMgSiO}_4 + \text{CaSiO}_3$, which under equilibrium conditions occurs at ~ 950 K [11]. Melilite-anorthite assemblages in 100, 160, and 6-1-72 are pseudomorphed by grossular, monticellite, and forsterite, indicating another isochemical reaction: $3\text{Ca}_2\text{MgSi}_2\text{O}_7 + \text{Ca}_2\text{Al}_2\text{SiO}_7 + 2\text{CaAl}_2\text{Si}_2\text{O}_8 = 3\text{Ca}_3\text{Al}_2\text{Si}_3\text{O}_{12} + \text{CaMgSiO}_4 + \text{Mg}_2\text{SiO}_4$. Although under equilibrium conditions, for melilite of Åk70, this reaction also occurs below 950 K, the common presence of unaltered melilite-anorthite intergrowths in the Allende Type C CAIs implies the lack of full equilibrium.

References: [1] Wark D. 1987. *GCA* 51: 221. [2] Beckett J. & Grossman L. 1988. *EPSL* 89: 1. [3] Aléon et al. 2002. *MAPS* 37: 1729. [4] Itoh et al. 2004. *GCA* 68: 183. [5] Lin Y. & Kimura M. 1998. *MAPS* 33: 435. [6] Krot et al. 2002. *MAPS* 37: 155. [7] Krot A. & Keil K. 2002. *MAPS* 37: 91. [8] MacPherson G. & Huss G. 2005. *GCA* 69: in press. [9] Krot et al. 2005. *ApJ* 622: 1333. [10] Krot et al. 2005. *Nature* 434: 998. [11] Hutcheon I. & Newton R. 1981. *LPSC* 12: 491.

LUNAR FELDSPATHIC METEORITE NWA 2200; A POLYMICT GLASSY IMPACT-MELT BRECCIA WITH FERROAN ANORTHOSITE (FAN) AFFINITIES. S. M. Kuehner¹, A. J. Irving¹ and D. A. Gregory². ¹Dept. of Earth & Space Sciences, University of Washington, Seattle, WA 98195 kuehner@u.washington.edu, ²St. Thomas, Ontario, Canada.

Introduction: A completely crusted 552 g ellipsoidal stone found in the Atlas Mountains, Morocco in 2004 consists of relatively large lithic and mineral clasts in a darker, very fine grained to glassy matrix. Sparse lithic clasts are mainly fine grained, feldspathic rocks containing equant grains of pyroxene and/or olivine from probable anorthositic to gabbroic precursors. A small percentage of the clasts are ophitic or quench-textured mare basalts. Mineral clasts identified by EDS include anorthitic plagioclase, olivine (~Fa₃₀₋₆₀), exsolved pigeonite, clinopyroxene, irregular grains of metal (with ~10-45 wt.% Ni), Ti-rich chromite, Ti-poor chromite, pyroxene-like glass(?) fragments, schreibersite (~5 wt.% Ni), ilmenite, troilite and zirconolite. FeO/MnO ratios measured by WDS for olivine (99.7, 105.5), clinopyroxene (73.7) and orthopyroxene (65.4) are unmistakably within the ranges for these minerals in known lunar rocks.

Mineral Compositions: Clinopyroxene and orthopyroxene grains in mineral and lithic clasts have $100\text{Fe}/(\text{Fe}+\text{Mg}) = 25.8-48.2$. Nineteen of 23 analyses have $\text{Ti}/(\text{Ti}+\text{Cr}) = 0.53-0.75$ and overlap the boundary defined by pyroxenes from highlands and high Ti-basalts on the summary diagram of [1]. The compositions of the other five pyroxenes suggest derivation from mare lithologies. Feldspar grains analyzed in mineral and lithic clasts have a narrow compositional range of $100\text{Ca}/(\text{Ca}+\text{Na}+\text{K}) = 95.8-97.4$. This combination of An-rich feldspars and relatively Fe-rich pyroxenes (Figure 1, [2]) demonstrates that most clasts are derived from ferroan anorthosite (FAN) lithologies.



References: [1] Kuehner, S. et al., 2005. LPS XXXVI #1228.
[2] Shervais, J. and Snow, C. 2002. LPS XXXIII, #1029.

TRACE ELEMENT ABUNDANCES IN ST. AUBIN (UNGR IRON) GIANT CHROMITE AND ASSOCIATED PHASES.

G. Kurat¹, E. Zinner² and M. E. Varela³. ¹Naturhistorisches Museum, Vienna, Austria. gero.kurat@univie.ac.at. ²Phys. Dept., Washington University, St. Louis, MO, USA. ³Dept. Geol., UNS-CONICET, B. Blanca, BA, Argentina.

Introduction: Chromite crystals of up to 3 cm in size were recently described from the fine octahedrite St. Aubin [1]. The crystals are euhedral exhibiting triangular and hexagonal cross sections and are incompletely covered by schreibersite, troilite and swathing kamacite. They are accompanied by schreibersite, troilite, hibbingite and euhedral Fe-phosphate (sarcopside or graftonite). We have analyzed the non-metallic phases for their major, minor and trace element contents with an EMP and an IMS-3f ion probe, which was also utilized to search for extinct ⁵³Mn in the Fe-phosphates – all following routine procedures.

Results: Chromite is pure FeCr₂O₄ containing (in ppm) ~8000 V, ~4700 Mn (but only ~600 Mg and ~0.4 Al), 0.15 Nb, 0.02 Sc and <0.003 Ce. The Fe-phosphate is also pure (Fe,Mn)₃(PO₄)₃ with (in ppm) ~18000 Mn, ~2000 Mg, ~270 Zn, 12.5 Cr, ~6 Co, 4.2 Ni, 0.01 Nb, 0.0017 Sc and ~0.0003 Ce. Hibbingite, Fe₂(OH)₃Cl (~18 wt% Cl), contains (in ppm) 6200 Ni, 2500 Co, 292 Mn, 0.0003 Sc and 0.0005 Ce. Fe-phosphates have excesses in ⁵³Cr with an initial ratio of ⁵³Mn/⁵⁵Mn = (1.5+/-0.3)x10⁻⁶.

Discussion: All non-metallic phases in St. Aubin are extremely poor in lithophile elements. Particularly striking are the very low contents of Al, Mg, Sc and Ti in chromite as compared to those reported by, e.g., [2]. Also, the contents of Zr and the REE are very low, all <0.01xCI. We interpret this to indicate derivation of the chromite from an environment that was very poor in all these elements. The same holds for the Fe-phosphate. Chromite and phosphate are also very poor in Ni, less so in the less siderophile Co, indicating equilibration with metal. On the other hand, chromite and phosphate are enriched in V and Nb and also Zn and Mn with respect to the common lithophile elements, indicating an elevated siderophile behavior of V and Nb – as was predicted by [3] - and formation of chromite and phosphate from reduced precursor phases. Hiddingite likely is a secondary phase after lawrencite and indicates also low abundances of lithophile elements during formation of the latter in the presence of metal.

Conclusion: All non-metallic phases in St. Aubin indicate formation in an environment that was very poor in lithophile elements. The abundance anomalies in V and Nb indicate reduced precursor phases (metals, carbides, etc.), which subsequently were oxidized to form chromite and Fe-phosphate early in the history, about contemporaneously with the Mn-Fe metasomatism event experienced by the angrites [4], while some ⁵³Mn still was alive. Thereafter, troilite and schreibersite formed, followed by lawrencite and final metal which preserved all phases.

Acknowledgements: We thank Andrey Gurenko and Nora

Groschopf, Mainz, for permission to use and help with the EMPA, respectively; financial support was received in Austria from FWF, the Academy of Sciences and the Freunde des NHM in Wien, in Argentina from CONICET, and in the USA from NASA.

References: [1] Fehr and Carion 2004. MAPS 39, A139-A141. [2] Bunch et al. 1970. Contr. Mineral. Petrol. 25, 297-340. [3] Jurewicz et al. 1995. EPSL 132, 183-198. [4] Lugmair and Shukolyukov 2002. MAPS 37, 1001-1013.

A ZONED SPINEL GRAIN IN THE FOUNTAIN HILLS BENCUBBINITE: CONSTRAINTS ON ITS THERMAL HISTORY.

A. R. La Blue¹, D. S. Lauretta¹, and M. Killgore².
¹Lunar and Planetary Laboratory, University of Arizona, Tucson, AZ. (arlablue@lpl.arizona.edu). ²Southwest Meteorite Laboratory, Payson, AZ.

Introduction: Fountain Hills (FH) is a metal-rich chondrite with abundant, well-defined chondrules. It contains important information about the processing of rocky and metallic material in the solar nebula. It was originally classified as a CB_a chondrite by [1] based on its O-isotopic composition and metal and silicate compositions. However, FH has similarities to both the CR and CB groups, suggesting that it is transitional between the two.

Thermal History: Mineralogy and major features of FH are described in a companion abstract [2]. An anorthite-rimmed, zoned spinel grain is present in FH with composition Mg_{0.9}Fe_{0.1}(Al_{0.9}Cr_{0.1})₂O₄. Cr and Ti increase systematically from core to rim while Al correspondingly decreases. The Mg/Fe ratio is constant at Mg# = 94. The area around the spinel is composed of anorthite and olivine. The nearest olivine crystal is 82 μm from the spinel. Since olivine is homogenous throughout FH, we assume it equilibrated with the rim of the spinel. We apply the olivine-spinel geothermometer (olv-sp) of [3] and calculate a temperature of 878 °C.

The composition of the spinel suggests that Mg and Fe were able to diffuse into the spinel and achieve equilibrium. The Cr and Al profiles suggest that diffusion in this system was sluggish and equilibrium was not achieved. This fact allows us to constrain the duration of heating experienced by FH. Cr-Al interdiffusion data for a spinel of composition Mg_{0.5}Fe_{0.5}(Al_{0.7}Cr_{0.3})₂O₄ have recently been measured at 21.4 kb and 1125°C [4], which suggest $D_{Cr-Al} = \sim 0.04 * D_{Fe-Mg}$. Using this relationship and the Arrhenius relation for D_{Fe-Mg} in spinel [5] we estimate D_{Cr-Al} in spinel at 878 °C. A reasonable fit to the data is obtained by treating the system as an isothermal diffusion problem. This analysis suggests a heating duration of ~1,800 years at 878 °C to establish the Cr-Al zoning in the FH spinel grain.

Discussion: The olv-sp temperature of 878°C represents closure of diffusive exchange between the spinel and olivine. We assume that it also represents closure between spinel and the Cr source (most likely metal). The diffusion calculations limit the duration of heating to ~1,800 years at 878°C. Similar calculations show that the grain could have been held at 600°C for 1.4 million years and at 400°C for over 5 billion years.

The short duration of peak heating may result from impact. Other bencubbinites have experienced significant shock metamorphism. However, olivine in FH exhibits sharp optical extinction indicating no shock features. FH could have been located near the surface of the asteroid when the impact occurred then ejected into free space post-impact which could explain the short heating. Shock features may have been erased during a period of lower temperature post-shock annealing [6].

References: [1] Lauretta et al. (2004) *LPSC* **35** #1255. [2] Lauretta et al (2005) *This meeting* [3] Sack and Ghiorso (1991) *Am. Min.* **76**, 827-847. [4] J. Ganguly, personal communication, 7/27/04. [5] Liermann and Ganguly (2002) *GCA* **66**, 2903-2913. [6] Rubin AE (2003) *LPSC* **34** #1262.

MÖSSBAUER STUDY OF IRON PHOSPHIDES EXTRACTED FROM SIKHOTE-ALIN METEORITE.

M.Yu. Larionov, V.I. Grokhovsky and M.I. Oshtrakh. Faculty of Physical Techniques and Devices for Quality Control, Ural State Technical University – UPI, Ekaterinburg 620002, Russian Federation. E-mail: lmur2000@rambler.ru, grokh47@mail.ru, oshtrakh@mail.utnet.ru.

Introduction: The iron nickel phosphides $(\text{Fe,Ni})_3\text{P}$ are occurred in iron meteorites in the forms of schreibersite and rhabdite. Schreibersite and rhabdite are formed as a result of heterogeneous and homogeneous nucleation mechanisms, respectively. A comparison of the hyperfine parameters of these phosphides is of interest due to differences of its nature.

Methods: The sample of schreibersite was prepared as a powder using mechanically extracted massive schreibersite from Sikhote–Alin meteorite (IIB) that was treated with HCl to remove kamacite residue. The small rhabdite crystals were extracted electrochemically from Sikhote–Alin meteorite (IIB) and used for sample preparation. Mössbauer spectra were measured at room temperature using Mössbauer spectrometer SM–2201 with high accuracy, stability and sensitivity in transmission geometry with moving absorber.

Discussion: Mössbauer spectra of schreibersite and rhabdite samples are shown in Fig. 1. These spectra appeared to be quite different. Mössbauer spectrum of schreibersite is very complicate and may consist of at least several magnetic sextets and several quadrupole doublets. A small amount of kamacite was not removed from the sample and related to very weak left and right outside peaks. Mössbauer spectrum of rhabdite demonstrates the presence of unresolved magnetic splitting and possibly quadrupole doublet. The unresolved magnetic splitting may be a result of the relaxation processes or fuzzy magnetic phase transition in the sample at room temperature as well as a result of superparamagnetic behavior of small rhabdite particles. These results demonstrate the difference of the hyperfine interactions in schreibersite and rhabdite related to its structure. However, further studies are required for detailed clarification.

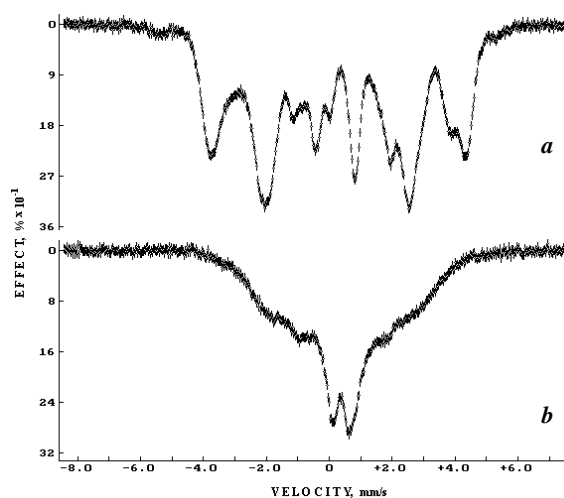


Fig. 1. Mössbauer spectra of schreibersite (*a*) and rhabdite (*b*). $T=295$ K.

THE FOUNTAIN HILLS BENCUBBINITE: A RECORD OF CHONDRULE FORMATION IN HIGH TEMPERATURE REGIONS OF THE SOLAR NEBULA. D. S. Lauretta¹, A. R. La Blue¹, and M. Killgore². ¹Lunar and Planetary Laboratory, University of Arizona, Tucson, AZ. (lauretta@lpl.arizona.edu). ²Southwest Meteorite Laboratory, Payson, AZ.

Introduction: The Fountain Hills (FH) meteorite was initially classified as a Bencubbin-like chondrite [1] based on its O-isotopic and mineral compositions. Here we describe the mineralogy and petrology of FH and explore implications for chondrule formation in high-temperature regions of the solar nebula.

Mineralogy and Bulk Composition: The modal mineralogy of Fountain Hills was estimated by correlating mineral compositions with elemental X-ray maps. We estimate that FH is composed of 43 wt.% metal, 22 wt.% low-Ca pyroxene, 16 wt.% olivine, 15 wt.% high-Ca pyroxene, 3.9 wt.% anorthite, and <0.15 wt.% sulfide and contains <2.5 vol.% void space.

Most metal occurs interstitial to chondrules and silicate fragments. It forms a near-continuous network of veins and rims that encase silicate grains. Small, metal grains in porphyritic chondrules are slightly Ni-rich. Olivine (from Fo₉₆ to Fo₉₈) occurs in barred and porphyritic chondrules and as isolated coarse grains dispersed throughout the sample. Low-Ca pyroxene (from En₈₉ to En₉₅) occurs predominantly as rims surrounding barred-olivine chondrules, porphyritic-olivine chondrules, and isolated olivine grains. High-Ca pyroxene (En₅₅Wo₄₁ to En₈₂Wo₁₅) occurs in barred, porphyritic, and granular chondrules. Plagioclase in Fountain Hills rim is extremely alkali-poor (An₉₉) and occurs almost exclusively in barred-olivine chondrules, interstitial to the olivine. In addition, anorthite occurs as a rim around isolated spinel grains [2].

Chondrule Petrology: FH contains abundant well-defined chondrules which range in size from 400 μm to 4200 μm in diameter and average ~1300 μm. Chondrule size correlates with texture. The largest chondrules (1200 – 4000 μm) and chondrule fragments have barred-olivine textures. Porphyritic olivine chondrules typically have smaller diameters (~1500 μm). Pyroxene-rich chondrules have radial and granular textures and are much smaller (average diameter = 800 μm).

Discussion: Recent studies of CB and CH chondrites suggest that their component chondrules and metal grains are pristine nebular condensates [3-4]. Evidence for this process includes chemical zonation in metal, absence of porphyritic and granular chondrules, and the high abundance of barred-olivine and cryptocrystalline chondrules. The lack of sulfide minerals and low alkali abundances are consistent with FH chondrule formation in a high-temperature region of the solar nebula. However, direct condensation of chondrule melts is inconsistent with observed chondrule textures. The formation of porphyritic chondrules requires either solid chondrule precursors or a large amount of dust to form nucleation sites in the chondrule melt. Thus, the presence of porphyritic and granular chondrules in FH suggests that these chondrules formed by: (1) incomplete melting of solid precursors or (2) melt formation in the presence of dust grains. The lack of fine-grained matrix in FH rules out (2). FH chondrules may have formed by processing of an earlier generation of CB chondrules.

References: [1] Lauretta et al. (2004) *LPSC 35* #1255. [2] La Blue et al. (2005) *This meeting*. [3] Meibom, A., et al. (1999). *JGR-Planets* **104(E9)**, 22053-22059. [4] Petaev, M. I. et al. (2001). *MAPS* **36**, 93-106.

THE LUNAR PROSPECTOR GAMMA-RAY AND NEUTRON SPECTROMETERS: OVERVIEW OF LUNAR GLOBAL COMPOSITION MEASUREMENTS. D. J. Lawrence¹, R. C. Elphic¹, W. C. Feldman¹, O. Gasnault², J. J. Hager¹, S. Maurice², T. H. Prettyman¹, ¹Los Alamos National Laboratory, Los Alamos, NM. E-mail: djlawrence. ²Centre d'Etude Spatiale des Rayonnements, Toulouse, France.

Introduction: The Lunar Prospector spacecraft orbited the Moon for 18-months starting in January 1998, and as part of its payload, it carried the Los Alamos-built neutron and gamma-ray spectrometers (LP-NS, LP-GRS). The scientific goals of the LP-NS and LP-GRS were to measure the global elemental composition of the Moon for a variety of geochemically important elements including H, Fe, Ti, Mg, Al, Si, Th, K, Gd, and Sm. While analysis of these data continue to produce new results [e.g., 1], previous studies have already provided a wealth of information about lunar formation and evolution processes as well as techniques and insight for interpreting orbital gamma-ray and neutron data.

Initial Results from the LP-NS and LP-GRS: Two of the major initial results from the LP-NS and LP-GRS were the mapping of enhanced hydrogen abundances at the poles of the Moon, and the global mapping of thorium and rare-earth elements abundances. By analyzing the LP-NS data, Feldman et al. [2] determined that the poles of the Moon have enhanced hydrogen abundances and in some locations this hydrogen may be in the form water ice. The global maps of thorium and the rare-earth elements Gd and Sm [3, 4] delineated for the first time the full extent of what is now called the Procellarum KREEP Terrane (PKT) [5].

Ongoing Work: Ongoing LP-NS and LP-GRS work covers two main categories: 1) Improved analysis of neutron and gamma-ray data for obtaining estimates of elemental abundances; and 2) interpretive studies of abundance data for understanding issues of lunar formation and evolution processes. The primary area of ongoing data analysis concerns the improvement of elemental abundance estimates for Fe, Ti, Th, K, Mg, Al, and Si of Prettyman et al. [6]. As presented by Prettyman et al. [7], nuclear physics databases (e.g., gamma-ray production probabilities) have been the primary source of uncertainty for these abundance estimates. However, revised analyses show a very good correspondence between sample and remotely sensed elemental abundances for Fe, Ti, Al, Th, K, and Mg. Interpretative studies of LP data have focused on delineating regions that have a significantly different composition from what is known from lunar samples. Regions of interest contain highly evolved lithologies [1, 8], mare basalts with high iron and thorium abundances, and Mg-rich regions [7].

References: [1] Hager¹, J. J. et al., *Met. and Planet. Sci.*, this meeting; [2] Feldman et al., *J. Geophys. Res.*, 106, 23,231, 2001; [3] Lawrence, D. J., et al., *J. Geophys. Res.*, 108, 10.1029/2003JE002050, 2003; [4] Elphic, R. C., et al., *J. Geophys. Res.*, 105, 20,333, 2000. [5] Jolliff, B. L., et al., *J. Geophys. Res.*, 105, 4197, 2000; [6] Prettyman, T. H., et al., *The Moon Beyond 2002: Next Steps in Lunar Science and Exploration*, 2002; [7] Prettyman, T. H., et al., *Europ. Geosci. Union*, EGU05-A-10067, 2005; [8] Lawrence, D. J., et al., *Geophys. Res. Letters*, 10.1029/2004GL022022, 2005.

MULTIPLE NAKHLITE LAVA FLOWS? R.C.F. Lentz¹, T.J. McCoy² and G.J. Taylor¹. ¹HIGP, Univ. of Hawaii, Honolulu, HI 96822. rclentz@higp.hawaii.edu. ²Dept. of Mineral Sciences, Nat'l Museum of Natural History, Smithsonian Inst., Washington D.C. 20560-0119.

Introduction: With the identification of MIL 03346 there are now seven nakhlites, offering more details to unravel the history of these unusual rocks. Many authors [e.g. 1] have recognized correlated progressions of several characteristics (e.g. ol and px core compositions, zoning profiles, mesostasis texture and abundance, CSD turnover) that suggest a stratigraphic order to the nakhlites within a cooling pile. However, the situation may be more complicated, as we discuss here.

Olivine texture and abundance: While it is not unusual for olivine distribution within a flow to vary due to crystal settling [2] or flow accumulation [3], these processes usually lead to predictable patterns of sizes and relative abundances of phenocrysts in different horizons. However, when we examine the texture and distribution of olivine among the seven nakhlites, there is no well-defined correlation with the assumed stratigraphic order. For example, the two newest nakhlites, MIL 03346 and NWA 817, both cooled rapidly (steep zoning profiles in ol and px, glassy mesostasis lacking the traditional plagioclase sprays), suggesting shallow, and nearby, emplacement. However, MIL has large, partly poikilitic, olivine grains (avg width = 720 μ m) but in very sparse numbers (0.02/mm²), while NWA 817 has smaller olivine grains (avg width = 364 μ m) in far greater density (0.45/mm²). We also find that those meteorites (Lafayette and NWA 998) with the greatest grain density (1.0/mm²) have the smallest average olivine sizes (279 μ m and 245 μ m, respectively). This correlation suggests a nucleation effect, rather than depth dependence governed by phenocryst settling or flow accumulation. We propose that the different textures and distributions of olivine are primary features that reflect formation of the nakhlites in two or more related flows. Slight variations in composition would then cause the differences in olivine abundance as it grew in clusters with surrounding pyroxene. Based on our measurements, we suggest preliminary flow groupings of (1) NWA 817, Nakhla, and Governador Valadares and (2) Y593/479, Lafayette, and NWA 998. MIL 03346 is dissimilar to both groups and may represent yet another flow. Multiple source flows implies a complex flow field and magma system, consistent with the newly suggested source region of Syrtis Major [4], rather than one random, odd flow.

Missing Lithologic Unit: Comparison of bulk rock nakhlite compositions to likely parent magma compositions shows a missing basaltic component. The terrestrial analog, Theo's Flow, which shares numerous textural and compositional features with the nakhlites, has a 60-m pyroxenite overlain by a 40-m gabbro. This implies that if the nakhlites formed similarly, they could have been buried beneath some thickness of unsampled gabbroic material, creating a quandary for the rapid cooling of MIL and NWA 817. Perhaps these rocks represent late, viscous squeeze-outs from inflated lava flows, after pyroxene formed but before plagioclase saturated sufficiently to nucleate within the mesostasis.

References: [1] Treiman A.H. 2005. *Chemie de Erde* 65, in press. [2] Walker D. et al. 1976. *Proceedings of Lunar & Planetary Science Conference VII*: 1365-1389. [3] Komar P.D. 1972. *Geological Society of America Bulletin* 83: 973-987. [4] Harvey R.P and Hamilton V.E. 2005. Abstract #1019. 36th Lunar & Planetary Science Conference.

NOBLE GASES IN METEORITE SHOWERS FROM QUEEN ALEXANDRA RANGE AND FRONTIER MOUNTAIN.

Ingo Leya¹ and Kees C. Welten², ¹Physikalisches Institut, University of Bern, Sidlerstrasse 5, CH-3012 Bern, Switzerland, ²Space Science Laboratory, University of California, CA 94720, Berkeley, USA. E-mail: Ingo.Leya@phim.unibe.ch.

Introduction: Compared to iron meteorites, large stony meteorites are relatively rare because large stony meteorites fragment during atmospheric entry, thereby producing large meteorite showers. For reasons not yet understood, large chondrites appear to have complex exposure histories with a first-stage exposure on the parent body. Such chondrite showers are interesting for various reasons. First, we have to answer the question whether complex exposure histories are simply more readily detected in large objects due to multi-nuclide studies on various aliquots or whether large objects are really more likely experience complex exposure [1,2]. Second, multi-nuclide studies in large objects enable testing model calculations for cosmogenic nuclide production. Such models are usually validated either on terrestrial simulation experiments or on well studied meteorites. However, in both cases the “standards” are of average size, *i.e.* a size range of 40 – 50 cm. Therefore, large meteorites enable testing the models at the limit of their performance.

Experimental: We analyzed 8 samples from 4 different fragments of the QUE 90201 L/LL5 chondrite shower (radius ~ 80-100 cm) and 6 fragments from the FRO 90174 H3-6 chondrite shower (radius ~ 150 cm). Samples consisted of one or several chips (30 – 230 mg), free of fusion crust, wrapped in Ni-foil. Prior to analysis, samples were preheated to desorb loosely bound atmospheric contamination. He, Ne and Ar were measured.

Results: Duplicate analyses on small chips of the same fragment generally give reproducible He and Ne concentrations, whereas the Ar concentrations show more scatter. The scatter in the Ar results is mainly due to different amounts of adsorbed atmospheric Ar. *Results for QUE-samples:* Concentrations of cosmogenic ³He and ²¹Ne vary by only a factor of 2-4. The (³He/²¹Ne)_c ratio ranges from 1.6 to 4.6, while the ²²Ne/²¹Ne ratio ranges from 1.02 to 1.06. The narrow range in ²²Ne/²¹Ne is similar to those observed in other large objects, such as Gold Basin [1] and Jilin [3], whereas larger variations would be expected for the ²¹Ne concentrations. For example, the ²¹Ne concentrations measured in 18 different Gold Basin fragments varies by a factor of 30 [1]. Surprisingly, some QUE samples show ²²Ne/²¹Ne ratios as low as 1.02 – 1.03, *i.e.* significantly lower than the ratio of 1.06 assumed so far as a lower limit for the shielding parameter. The ³⁸Ar concentration varies by a factor of 2-3 and for some samples an elevated ³⁶Ar/³⁸Ar were found. *Results for FRO-samples:* The ²¹Ne and ³He concentrations vary by factors of 6.1 and 6.3 respectively. Some FRO fragments show solar contributions to the Ne isotopes, which compromise detailed studies of the cosmogenic ²²Ne/²¹Ne ratio.

The noble gas data together with radionuclide data are presented and the exposure histories of the QUE 90201 and FRO 90174 chondrite showers are discussed.

References: [1] Welten et al. 2003, *Meteoritics & Planetary Sciences* 38, 157-173. [2] Welten et al. 2004. Abstract #2020, 35th Lunar & Planetary Science Conference. [3] Begemann et al. 1996, *Meteoritics & Planetary Sciences* 31, 667-674.

TITANIUM ISOTOPES IN THE SOLAR SYSTEM.

I. Leya¹, M. Schönbächler², U. Wiechert³, A.N. Halliday⁴.
¹Physikalisches Institut, University of Bern, Sidlerstrasse 5, CH-3012 Bern, Switzerland, ²Carnegie Institution of Washington, Washington DC, USA, ³Institute for Isotope Geology, ETH Zürich, Switzerland, ⁴Departement of Earth Sciences, University of Oxford, Oxford, UK. E-mail: Ingo.Leya@phim.unibe.ch

Introduction: Isotopic anomalies in solar system objects provide powerful constraints on the origin and evolution of the early solar system. To a large degree, the solar system is surprisingly homogenous isotopically, indicating very efficient mixing. Exceptions are isotopic anomalies due to *in situ* effects such as radioactive decay and particle irradiation. Therefore, isotopic anomalies indicating incomplete homogenization are of great importance for understanding processes in the early solar system. Isotopic anomalies have been known for many years for *e.g.*, noble gases, O, Ti, Cr, Zr, Sm, Nd, and Ba.

Here we present first results of our study of the Ti isotopic compositions of solar system objects. The goal of this study is two-fold *i*) to determine the Ti isotopic compositions in various solar system objects and search for anomalies in early refractory condensates to further proof or reject the hypothesis that some of the short-lived radionuclides have been produced by particle irradiation and *ii*) to add Ti to the list of elements measured via high resolution MC-ICPMS.

Experimental: Sample preparation and chemical separation is described in [1]. All isotopic measurements were performed on the high sensitive high resolution MC-ICPMS at the ETH Zürich (Nu1700). The mass resolution was always about 2000 to resolve interferences on ⁵⁰Ti from, *e.g.*, ¹⁴N³⁶Ar. Interferences on ⁵⁰Ti by ⁵⁰V and ⁵⁰Cr and on ⁴⁶Ti by ⁴⁶Ca are corrected via ⁵¹V, ⁵³Cr and ⁴⁴Ca, respectively. Interferences from doubly charged Zr and Mo were corrected via measured Zr/Ti and Mo/Ti ratios and experimentally determined Zr²⁺/Zr⁺ and Mo²⁺/Mo⁺ ratios. Mass dependent fractionation is corrected internally via ⁴⁹Ti/⁴⁷Ti.

Results: Surprisingly, all Ti standard solutions yield ⁵⁰Ti/⁴⁷Ti ratios about 12 ε-units higher than the reference value given by [2]. The grand average for ⁵⁰Ti/⁴⁷Ti, ⁴⁸Ti/⁴⁷Ti and ⁴⁶Ti/⁴⁷Ti is 12.76 ± 0.32, -0.37 ± 0.14 and 2.36 ± 0.42 ε-units (2σ-uncertainties) relative to the values given by [2]. The 12 ε-unit offset does neither depend on the concentration of the analyzed standards nor on the set-up used for measurement. Therefore, the offset for the terrestrial ⁵⁰Ti/⁴⁷Ti is most probably not an experimental artifact and one has to consider the possibility that the terrestrial ⁵⁰Ti/⁴⁷Ti ratio might be off by 12 ε-units relative to the value given by [2]. The external reproducibility (2σ) for ⁵⁰Ti/⁴⁷Ti, ⁴⁸Ti/⁴⁷Ti and ⁴⁶Ti/⁴⁷Ti is 0.32, 0.14 and 0.42 ε-units, respectively.

The results for lunar samples and bulk meteorites indicate that the Ti isotopic composition is strikingly uniform. Neither lunar whole rock samples nor any of the mineral separates show any deviations from terrestrial. Isotopic anomalies for ⁵⁰Ti/⁴⁷Ti have only been found for CAIs (which is expected) and Estacado troilites. However, this is an ongoing study and more results will be presented at the conference.

References: [1] Schönbächler M. et al. (2004) *Analyst*, 129, 32-37. [2] Niederer F.R. et al. *GCA*, 49, 835-851.

MAJOR TRACE AND PLATINUM-GROUP ELEMENTS OF THE MARTIAN LHERZOLITE GROVE MOUNTAINS (GRV) 99027. Yangting Lin¹ Liang Qi², Quiqing Wang³, Lin Xu⁴. ¹State Key Laboratory of Lithospheric Evolution, Institute of Geology and Geophysics, Chinese Academy of Sciences, Beijing 100029, China, LinYT@mail.igcas.ac.cn; ²Department of Earth science, The university of Hong Kong; ³Guangzhou Institute of Geochemistry, Chinese Academy of Sciences; ⁴National Astronomic Observatory, Chinese Academy of Sciences, Beijing.

Introduction: As a part of a systematic study of the martian lherzolite GRV 99027, a bulk sample of 39.6 mg and a fine-grained fraction (<50 μm) of 39.2 mg were analyzed for major elements by inductively coupled plasma atomic emission spectrometry (ICP-AES), and for trace elements by inductively coupled plasma mass spectrometry (ICP-MS). Another bulk sample of 104.7 mg was digested using Carius tube technique, and platinum-group elements (PGEs) were determined by ICP-MS.

Results: Analyses of the bulk sample and fine-grained fraction of GRV 99027 show significant variations. Concentrations of Al, Ti, Cr, P, U, Th, Y and REE are higher in the fine-grained fraction than in the bulk sample, reflecting higher modal abundances of plagioclase, Ti-chromite, ilmenite and phosphates in the former than the latter. This is because that plagioclase is easier to be grinded down than olivine and pyroxenes, and Ti-chromite, ilmenite and phosphates always coexist with plagioclase in the interstitial region of the meteorite [1]. Refractory lithophiles (Ca, Sc, Zr, Hf) and moderate siderophiles (Fe, Co, Ni, Cu, Ge) are closely similar between the bulk and fine-grained samples.

The bulk GRV 99027 has a "hump" shape of REE pattern increasing from La ($0.84 \times \text{CI}$) to Dy ($3 \times \text{CI}$), and then decreasing to Lu ($2.2 \times \text{CI}$), without Ce or Eu anomaly. The REE pattern is nearly parallel to those of other martian lherzolites, *i.e.* ALHA77005, Y-793605 and LEW 88516 [2-4], except for significant variation in Ce values between the literature datasets. The REE concentration of GRV 99027 is lower than those of ALHA77005 and LEW 88516, but slightly higher than that of Y-793605. However, this difference could be due to heterogeneity of the samples, as indicated by the variations between the bulk and fine-grained samples of GRV 99027. Other elements also show close similarity between these martian lherzolites, except for their large disagreements in U and Th values.

The Os/Ir ratio of GRV 99027 is chondritic ($1.03 \times \text{CI}$), and all of Os, Ir, Ru, Pt and Rh show a nearly flat pattern with $0.004\text{-}0.008 \times \text{CI}$. Enrichments of Pd, Ni and Co increase to 0.018 , 0.029 , and $0.13 \times \text{CI}$, respectively. In comparison with Y-793605 and ALH 77005 martian lherzolites [4], GRV 99027 contains slightly lower concentrations of PGEs without negative Pt anomaly.

Acknowledgements: We thank Ying Liu, Guangqian Hu and Xianglin Tu for laboratorial assistances for major and trace element analyses. The sample is provided by the Polar Research Institute of China, and the study is supported by the Natural Science Foundation of China (Grant No. 40232026).

References: [1] Lin Y., et al. 2003. *Chinese Science Bulletin* 48: 1771-1774. [2] Shih C. Y., et al. 1982. *Geochimica et Cosmochimica Acta* 46: 2323-2344. [3] Gleason J. D. 1997. *Geochimica et Cosmochimica Acta* 61: 4007-4014. [4] Ebihara M., et al. 1997. *Antarctic Meteorite Research* 10: 83-94.

RE-EXAMINATION OF ^{26}Al ABUNDANCE IN CM HIBONITE GRAINS. Ming-Chang Liu¹ and Kevin D. McKeegan¹. ¹Dept. of Earth and Space Sciences, UCLA, Los Angeles, CA. E-mail: mcliu@ess.ucla.edu.

Introduction: Following the demonstration of the in situ nature of the decay of ^{26}Al in CAIs [1], a large number of Mg isotope measurements were performed by Secondary Ion Mass Spectrometry (SIMS) on mineral phases with high Al/Mg ratios, such as anorthite. The data indicate a prominent peak in $^{26}\text{Al}/^{27}\text{Al}$ relative abundance at $\sim 4.5 \times 10^{-5}$ and this “canonical” value has been thought to represent an initial ratio characteristic of wide regions of solar nebula at the time of formation of the first solid materials [2]. However, recent high-precision analyses of Mg isotopes of whole digested CAIs and in-situ laser ablation measurements carried out by Multiple Collection Inductively Coupled Plasma Mass Spectrometry (MC-ICPMS) have suggested a higher initial $^{26}\text{Al}/^{27}\text{Al}$ ratio of $\sim 7 \times 10^{-5}$ [3-6]. In this context, the previous canonical value would reflect isotopic closure $\sim 300,000$ years after CAI crystallization [6]. On the other hand, using similar techniques, Bizzarro and colleagues [7] find that all CAIs analyzed fall on a single Al-Mg isochron with $^{26}\text{Al}/^{27}\text{Al} = 5.2 \times 10^{-5}$, indicating that these objects formed contemporaneously within the first 50,000 years of the solar system. These data are essentially all from large CAIs from CV chondrites.

^{26}Al in Hibonite Grains: Hibonite, which is a dominant refractory phase in CM chondrites, is interesting in this regard because it is thought to represent one of the earliest solar system phases. Mg isotopes in CM hibonite grains have been studied by several authors revealing a complex pattern of initial $^{26}\text{Al}/^{27}\text{Al}$ abundances which are linked with petrographic characteristics [8-12]. Isolated platy hibonite crystals are typically devoid of measurable ^{26}Al , whereas spinel-hibonite inclusions (SHIBs) often show $^{26}\text{Al}/^{27}\text{Al}$ values that have been considered classically ‘canonical’ ($\sim 5 \times 10^{-5}$). The ^{26}Al data show a qualitative correlation with very short-lived ^{41}Ca [11, 12]. However, all these Mg isotope data were obtained by SIMS before the development of high-precision multiple collector ion probe techniques [e.g., 13]. A weighted fit to all published data for hibonites bearing resolvable $^{26}\text{Mg}^*$ and with Al/Mg <40 (mainly SHIBs), results in a fairly good correlation ($\chi^2=1.6$) on the Al-Mg evolution diagram with $^{26}\text{Al}/^{27}\text{Al} = (4.24 \pm 0.23) \times 10^{-5}$ but with a non-zero intercept ($=1.27 \pm 0.15\%$). Forcing the fit through the origin results in a steeper slope corresponding to $^{26}\text{Al}/^{27}\text{Al} = (5.14 \pm 0.12) \times 10^{-5}$ (1σ). In this sense, the CM hibonite data fit reasonably well with the scenario provided by the CV CAI data of Bizzarro et al. [7], however, it must be acknowledged that the analytical uncertainties are also large enough to accommodate a spread of apparent ages, possibly up to $^{26}\text{Al}/^{27}\text{Al}$ values approaching 7×10^{-5} for some individual samples. We are engaged in a new campaign to carry out Mg isotope analyses on additional CM hibonites by high-precision SIMS; initial results will be reported at the meeting.

References: [1] Lee et al. 1976. *GRL*: 41-44. [2] MacPherson et al., 1995. *Meteoritics*: 365-386. [3] Galy et al., 2000. *Science*: 1751-1754 [4] Young et al., 2002. *GCA*: 683-698. [5] Galy et al., 2004. *LPSCXXXV*: #1790 [6] Young et al., 2005. *Science*: 223-227 [7] Bizzarro et al., 2004. *Nature*: 275-278 [8] Fahey et al., 1987. *GCA*: 329-350. [9] Ireland 1988. *GCA*: 2827-2839. [10] Ireland 1990. *GCA*: 3219-3237. [11] Sahijpal et al., 2000. *GCA*: 1989-2005. [12] Marhas 2001. Ph.D dissertation. [13] McKeegan et al., 2004. *MAPS*: #5224

MORPHOLOGIES OF APOLLO 17 DUST AND LUNAR SIMULANT JSC-1. Yang Liu, Lawrence A. Taylor, Eddy Hill, James M.D. Day Department of Earth & Planetary Sciences, Planetary Geosciences Institute, University of Tennessee, Knoxville, TN 37996. E-mail: yangl@utk.edu

Introduction: Lunar dust (<20 μm) makes up ~20 wt.% of the lunar soil. Because of the abrasive and adhering nature of lunar soil, a detailed knowledge of the morphology (size, shape and abundance) of lunar dust is important for dust mitigation on the Moon. This represents a critical step towards the establishment of long-term human presence on the Moon [1]. Machinery design for in-situ resource utilization (ISRU) on the Moon also requires detailed information on dust morphology. Here we report a morphological study of dust sample 70051 and compare it to a lunar soil simulant (JSC-1).

Results: We have obtained SEM images of dust grains from sample 70051 soil. The dust grains imaged are mainly composed of fragments of minerals, rocks, agglutinates and glass with occasional glass spheres. Most particles imaged are partially coated with glass. Grains of a few μm are mainly agglutinates. All grains imaged show sub-angular to angular shapes. There are four prominent shapes: ropey shape (typical for agglutinates), shard, block, and 'Swiss-cheese' (high concentration of submicron bubbles). Submicron bubbles and cracks are present in most grains.

We also imaged dust grains of a lunar soil simulant (JSC-1), which was produced from a glass-rich basaltic tuff [2]. JSC-1 dust grains are angular blocks and shards, lacking the ropey and 'Swiss-cheese' shapes as well as submicron cracks and bubbles.

Discussion and Implications: The presence of submicron features (bubbles and cracks) may increase the effective surface area of dust grains, implying that lunar dust may be potentially important to ISRU, namely for the production of oxygen on the Moon and in harvesting solar wind from lunar soil. The lack of these features in JSC-1 indicates that corrections need to be made when using JSC-1 for ISRU experiments and contrasting these experiments with real lunar soil.

Methods of dust mitigation on critical surfaces such as the solar array and visor need to account for the sharp edges of lunar dust particles. In the case of textile surfaces, the irregular shaped dust particles can become trapped in fibers, making it difficult to remove them by brushing or using a gas blower. Particles with sharp edges can even work their way into deeper layers of the clothes, making them even more difficult to remove.

References: [1] Taylor L.A. *et al.* 2005, *1st Space Explor. Conf.*, AIAA. [2] McKay D. S. *et al.* 1994. *Space IV*, ASCE, 857-866. [3] Klosky J.L. *et al.* 1996. *Space V*, ASCE, 680-688.

SIMULATION OF NANOPHASE IRON IN LUNAR SOIL FOR USE IN ISRU STUDIES. Yang Liu, Lawrence A. Taylor, Eddy Hill, James M.D. Day Planetary Geosciences Institute, Department of Earth & Planetary Sciences, University of Tennessee, Knoxville, TN 37996. E-mail: yangl@utk.edu

Introduction: For the prospective return of humans to the Moon, large quantities of lunar soil simulants are required for technological development and medical testing due to the limited amount of lunar soil available on Earth. Since the Apollo era, there have been several simulants; of these JSC-1 and MLS-1 are widely used. JSC-1 was chosen for geotechnical tests because of its high glass content, while MLS-1 approximates the chemistry of Apollo 11 high-Ti soil 10084. Stocks of both simulants are depleted. The lunar soil simulant materials workshop, held in Colorado School of Mines in January 2005, identified the need to clone JSC-1 and to make new simulants for the special properties of lunar soil such as nanophase iron (np-Fe⁰).

Np-Fe⁰ in lunar soil: Lunar soil is formed by space weathering of lunar rocks (e.g., micrometeorite impact, interaction with solar wind). Glass generated during micrometeorite impact cements rock and mineral fragments to form agglutinates and coats soil grains. Taylor *et al.* [1] showed that the relative amount of impact glass in lunar soil increases with decreasing grain size and is the most abundant component in lunar dust (<20 μm fraction). Notably, the magnetic susceptibility of lunar soil also increases with the decreasing grain size. Keller *et al.* [2, 3] found the presence of np-Fe⁰ particles in the glass rim coatings. Therefore, the correlation of glass content and magnetic susceptibility can be explained by the presence of the np-Fe⁰ particles in glass: small particles contain relatively more np-Fe⁰ because of more glass coating the intrinsically larger surface areas.

A new simulant: We have prepared materials simulating np-Fe⁰ in the lunar glass by adapting the method of Allen *et al.* [4]. Silica gel with an average pore size of 6 to 15 nm was impregnated with iron nitrate solution and then dried after removing the extra solution by filtration. After repeating the impregnation step several times, iron nitrate in the pores of silica gel was reduced to form metallic iron using H₂ gas. XRD spectrum showed only α -Fe phase.

Discussion: The magnetic property of lunar soil is important in dust mitigation on the Moon [5]. Thus material simulating this property is important for testing mitigation methods using electromagnetic field. Ultimately, however, LRS with np-Fe⁰ need to be combined with other simulants in order to adequately approximate the chemistry and mineralogy of the lunar soil.

References: [1] Taylor L. A. *et al.* 2001, *Journal of Geophysical Research* **106** 27985-27999. [2] Keller L. P. and McKay D. S. 1997, *Geochimica Cosmochimica Acta* **61** 2331-2340. [3] Keller L. P. *et al.* 1999, *New views Moon II*. [4] Allen C. C. *et al.* 1996, 27th Lunar and Planetary Science Conference, 13-14. [5] Taylor L.A. *et al.* 2005, AIAA (submitted)